

THE QUANTUM MANY BODY PROBLEM

**JUST THE UNIVERSE MAKING IT HARD
FOR US TO PREDICT HER, OR RATHER
A FUNDAMENTAL LIMITATION?**

**BY
Xabier Oyanguren Asua**

Thesis Directors:

**Jordi Mompart Penina
Xavier Oriols Pladecall**

**Universitat Autònoma de Barcelona
DEGREE FINAL DISSERTATION
Bachelor's degree in Nanoscience and Nanotechnology
2019-2020**

Contents

1	The Problem	1
1.1	Decrypting the Schrödinger Equation: The two <i>real</i> equations composing it	1
1.2	Isn't this classical mechanics?!...Well, almost	2
1.3	Then, what am I really computing when using the Schrödinger Equation?	4
1.4	Why is it so hard to predict even just the motion of a single 1D particle?	5
1.5	The Literal Interpretation of Quantum Mechanics : An existential relief?	7
2	Trying to achieve the exactest numerical time evolution: the Crank-Nicolson algorithm	9
2.1	n=1: One spatial dimension	11
2.2	n=2: Two spatial dimensions (2 quantum 1D particles or a single 2D particle)	12
2.3	n=3 and n=N: Generalization of the CN matrix approach	12
2.4	How to solve the matrix equation?	13
2.5	The Actual Code Implementation	14
2.6	Computing Bohmian Trajectories using the Wavefunction	14
2.7	Simulation Examples: How Trajectories approximate the Probability Density	15
3	The Conditional Single Particle Wavefunction Decomposition: An exponential problem turned into polynomial?	18
3.1	The Conditional Single Particle Wavefunction Decomposition	18
3.2	Algorithm A: The Zero-th Order Taylor Expansion of G_a and J_a	19
3.2.1	Testing the Algorithm: The Double Slit Experiment	21
3.3	Algorithm B: The Born-Huang Expansion and Adiabatic States	22
3.3.1	The Born-Huang expansion and the Adiabatic States	22
3.3.2	Adiabatic states for the simple infinite wall geometric constriction	23
3.3.3	The Master Equation of the Algorithm: the Born-Huang expansion into the SE	23
3.3.4	Our Benchmark Problem	25
3.3.5	Testing $\chi^j(x, t)$ Quality	26
3.3.6	Testing if Correlations are Captured	27
3.3.7	Conclusions of the Tests	29
4	In a Nutshell	30
Supplementary Figures		31
Appendices		34
Appendix A: Grid Parameters for the Simulations of the Figures		34
Appendix B: Imaginary Time Evolution		35
Appendix C: Important Properties of the Adiabatic Coefficients		37
Appendix D: The Laplacian		38
Appendix E: Derivation of the Conditional Single Particle Schrödinger like Equations		39
References		42

The Quantum Many Body Problem

The exponential growth in complexity with increasing number of dimensions

Abstract

The dissertation that follows has been divided into three main sections: we will first envision the weight of the many body problem from a theoretical standpoint by trying to intuitively understand the difference between classical and quantum particle dynamics. We will then introduce a numerical method to solve the Schrödinger Equation with no theoretic approximation: the Cranck Nicolson method, which we will generalize to an arbitrary dimension. This will let us prove that the computational complexity grows exponentially, revealing now the problem from a practical standpoint and laying bare the need for approximations in temporal dynamics. A framework with this objective will be opened by the Conditional Wave Function decomposition. Two algorithms will be exposed and contrasted here: a first design developed in [14] (Alg.A) and a completely new algorithm in development (Alg.B), that will be implemented and tested here for the very first time.

1 The Problem

Any non-relativistic quantum system is fully described by a complex function $\Psi(\vec{q}, t)$, which takes n real spatial degrees of freedom $\vec{q} = \{q_j\}_{j=0}^n \in \mathbb{R}^n$ and an absolute time t . Its name is the **wavefunction**, and contains the information of any observable of the system. It turns out that its complex module squared $|\Psi(\vec{q}, t)|^2$ gives the probability density function to find the system at a certain point \vec{q} at a given time. The n spatial degrees of freedom use to represent the 3 Cartesian coordinates in the physical Euclidean 3-space of each of the bodies in the system. That is, if the system is composed of N “particles” then $n = 3N$. Nonetheless, a system of n 1D particles could equally be represented by such a wavefunction, or a system of M 2D particles such that $n = 2M$. Therefore, in general throughout the work, we will simply refer to the n spatial degrees of freedom as **dimensions**. Anyhow, if the n degrees of freedom represent all the particles in the Universe, then a point $(\vec{q}, t) \in \mathbb{R}^{n+1}$ in the so called **configuration space**, represents an instance of the Universe if all the “particles” were really discrete particles.

Let us introduce the main equation we will be dealing with for all the present work: the many-particle time dependent Schrödinger Equation (SE), which is the equation of motion governing the time evolution of the wave-function if the system is under the influence of a real scalar field called the *potential energy field* $V(\vec{q}, t)$:

$$i\hbar \frac{\partial \Psi(q_1, \dots, q_n, t)}{\partial t} = - \sum_{k=1}^n \frac{\hbar^2}{2m_k} \frac{\partial^2 \Psi(q_1, \dots, q_n, t)}{\partial q_k^2} + V(q_1, \dots, q_n, t) \Psi(q_1, \dots, q_n, t) \quad (\text{SE})$$

where m_k is the mass associated to the k -th degree of freedom, $i = \sqrt{-1}$ and \hbar is a constant with action units called the Planck constant.

1.1 Decrypting the Schrödinger Equation: The two *real* equations composing it

Why is it so hard to compute the dynamics of even a single 1D quantum particle? Long story short, it is just due to the fact that in contrast with classical Newtonian mechanics, it is necessary to evolve every single possible trajectory the particle could have simultaneously, as if each of the possible trajectories of the particle affected the rest. This is called the Quantum Wholeness [1]. Let us illustrate this statement with the following insightful derivation:

Let us write the wavefunction in polar form: $\Psi(\vec{q}, t) = R(\vec{q}, t)e^{S(\vec{q}, t)/\mu}$. Where we introduced a constant μ dividing the phase S , as the exponential must be unit-less. As we will see S has action units, then we could choose any constant with these units. Let us choose $\mu = \hbar$. Note how $R(\vec{q}, t) : \mathbb{R}^{n+1} \rightarrow [0, \infty) \subset \mathbb{R}$ and $S(\vec{q}, t) : \mathbb{R}^{n+1} \rightarrow [-\pi, \pi] \subset \mathbb{R}$, are both just *real* scalar fields (no more complex number stuff that “might be hard to physically imagine”). Then, let us introduce $\Psi(\vec{q}, t) = R(\vec{q}, t)e^{S(\vec{q}, t)/\hbar}$ in the Schrödinger Equation (SE):

$$i\hbar \frac{\partial R(\vec{q}, t)e^{S(\vec{q}, t)/\hbar}}{\partial t} = - \sum_{k=1}^n \frac{\hbar^2}{2m_k} \frac{\partial^2 R(\vec{q}, t)e^{S(\vec{q}, t)/\hbar}}{\partial q_k^2} + V(q_1, \dots, q_n, t)R(\vec{q}, t)e^{S(\vec{q}, t)/\hbar}$$

Using the chain rule two times, the fact that complex numbers are a field and twice the Leibniz rule, we arrive to an expression where as $\forall S \in \mathbb{R} e^{iS/\hbar} \neq 0$, we can simplify the exponentials at both sides and rearranging terms obtain:

$$\Leftrightarrow -\frac{R}{\hbar} \frac{\partial S}{\partial t} + i \frac{\partial R}{\partial t} = \frac{VR}{\hbar} + \sum_{k=1}^n \frac{\hbar}{2m_k} \left(\frac{R}{\hbar^2} \left(\frac{\partial S}{\partial q_k} \right)^2 - \frac{\partial^2 R}{\partial q_k^2} \right) + i \sum_{k=1}^n \frac{-1}{2m_k} \left(R \frac{\partial^2 S}{\partial q_k^2} + 2 \frac{\partial R}{\partial q_k} \frac{\partial S}{\partial q_k} \right)$$

The real part of the *lhs* must be equal to the real part of the *rhs*, the same for the imaginary part. This gives us two real partial differential equations:

$$\begin{cases} -\frac{R}{\hbar} \frac{\partial S}{\partial t} = \frac{VR}{\hbar} + \sum_{k=1}^n \frac{\hbar}{2m_k} \left(\frac{R}{\hbar^2} \left(\frac{\partial S}{\partial q_k} \right)^2 - \frac{\partial^2 R}{\partial q_k^2} \right) \\ \frac{\partial R}{\partial t} = \sum_{k=1}^n \frac{-1}{2m_k} \left(R \frac{\partial^2 S}{\partial q_k^2} + 2 \frac{\partial R}{\partial q_k} \frac{\partial S}{\partial q_k} \right) \end{cases}$$

Where by simple algebraic manipulation and using a reverse chain rule for the second equation we arrive to the following system of coupled real differential equations (DE-s):

$$\frac{\partial S(\vec{q}, t)}{\partial t} = - \sum_{k=1}^n \frac{1}{2m_k} \left(\frac{\partial S}{\partial q_k} \right)^2 - V(\vec{q}, t) - \sum_{k=1}^n \frac{\hbar^2}{2m_k R} \frac{\partial^2 R}{\partial q_k^2} \quad (\text{QHJE})$$

$$\frac{\partial R^2(\vec{q}, t)}{\partial t} = \sum_{k=1}^n \frac{\partial}{\partial q_k} \left(R^2 \frac{\partial S}{\partial q_k} \right) \quad (\text{CE})$$

Due to the analogy with the Classical *Hamilton Jacobi Equation*, we will call the first the *Quantum Hamilton Jacobi Equation* (QHJE). This way, S could be interpreted as Hamilton's Principal Action, and as such we could define a velocity field as:

$$v_k(q_k, \vec{q}_b, t) = \frac{1}{m_k} \frac{\partial S(\vec{q}, t)}{\partial q_k} \quad \forall k \in \{1, \dots, n\}$$

Then, noting that $R(\vec{q}, t)^2 = \Psi^\dagger \Psi = |\Psi|^2$ is the probability density, the velocity field definition would make the second DE a *Continuity Equation* (CE), or a local density conservation equation for the quantity R^2 . The important point here is to acknowledge that evolving the SE is equivalent to evolving these two real DE-s!. Let us define as the **Quantum Potential**:

$$Q(\vec{q}, t) := \sum_{k=1}^n Q_k(\vec{q}, t) := - \sum_{k=1}^n \frac{\hbar^2}{2m_k R} \frac{\partial^2 R(\vec{q}, t)}{\partial q_k^2} \quad (\text{Q})$$

This term, will be the only term not present in Classical Mechanics!. Our aim in this section will be to intuitively understand these two real equations and prove their match with classical mechanics.

1.2 Isn't this classical mechanics?!...Well, almost

An immediate interpretation of these two equations comes from classical discrete mechanics. Here, given a system of n particles (n one dimensional particles or N 3D particles s.t. $n = 3N$) we have one main axiom: that the trajectory followed by the system of particles is such that the *action functional* \mathbb{S} is minimized (the **Action Principle**). That is, given two end-points $\vec{q}(t = t_0) = \vec{q}_A \in \mathbb{R}^n$ and $\vec{q}(t = t_f) = \vec{q}_B \in \mathbb{R}^n$, along all the possible curves connecting them, the physical trajectory the system will follow is the one extremizing the value of the action integral:

$$\mathbb{S}(\vec{q}(t)) = \int_{t_0}^{t_f} L(\vec{q}(t), \dot{\vec{q}}(t), t) dt \quad (\text{AP})$$

Note that now q_j are dependent variables with respect to time. They now define curves that depend on time and not absolute or independent degrees of freedom. We call **trajectory** of the system of n particles to such an n dimensional point moving in time: $\vec{q}(t)$.

In Classical Mechanics (CM), we talk about *discrete* point like particles. Thus, the idea of *trajectory* (a one dimensional manifold in \mathbb{R}^{n+1}) is the basic conception to describe the history of the system.

In contrast, in Quantum Mechanics (QM), the equation of motion describes a field, a wave, rather than a discrete ontological substrate. Each spatial degree of freedom is a time independent variable. In particular, we will see that $R(\vec{q}, t)^2$ appears to describe a continuous distribution of particles along each of the q_k degrees of freedom. Then, why do we still call the bodies particles? In QM, while the system of bodies is not observed, they appear to evolve as if each body was a continuous wave (SE), but when the system is measured, suddenly only point-like particles are found there. Thus, even if in QM, each ontological entity is no longer discrete in the time evolution or interactions, we still call them “particles”: when observed, only a discrete point like entity appears to be there.

The remaining main axioms of discrete CM are assuming certain non-relativistic symmetries about space-time¹. Using these symmetries, it can beautifully be derived from the **AP** [4], that the Lagrangian function ruling the motion must have the shape:

$$L(\vec{q}(t), \dot{\vec{q}}(t), t) = T(\dot{\vec{q}}(t)) + U(\vec{q}(t), t)$$

where T is the Kinetic Energy of the system and U the potential energy introducing constraints and correlations between the dimensions. It can also be shown [3] that the variational principle **AP** is fulfilled when the *Euler-Lagrange Equations* are followed for the particular shape of the Lagrangian, which in turn particularize to *Newton's Second Law*.

Now, even if everything seems to be described in terms of trajectories, in classical mechanics we can still find a *wave* that contains the information of all the possible trajectories. Defining *Hamilton's Principle Function S* as setting to the action functional parameters (\vec{q}, t) as the upper fixed point and leaving unspecified the lower fixed point:

$$S(\vec{q}, t) = \int_{t_0; \vec{q}(t_0)=q_0}^{t; \vec{q}(t)=\vec{q}} L(\vec{q}(t), \dot{\vec{q}}(t), t) dt$$

It can be shown [1] that this wave contains the information of the velocity field governing all the trajectories. In particular, given an initial point for the system $\vec{q}(t = t_0) = \vec{q}_A$, the trajectory of the system can be evolved using the velocity field given by:

$$\frac{dq_k(t)}{dt} = v_k(q_k(t), \vec{q}_b(t), t) = \frac{1}{m_k} \frac{\partial S(q_k, \vec{q}_b(t), t)}{\partial q_k} \Big|_{\vec{q}(t)} \quad \forall k \in \{1 \dots n\} \quad (\text{GL})$$

Let us call this the *Guidance Law* for the system of particles.

It can be shown as well [1], that by manipulating the **AP**, if the Lagrangian has the particular shape stated above, then the dynamics of the system follow in terms of the $S(\vec{q}, t)$, an equivalent DE to the Euler-Lagrange solution, called the classical *Hamilton Jacobi Equation*:

$$\frac{\partial S(\vec{q}, t)}{\partial t} = - \sum_{k=1}^n \frac{1}{2m_k} \left(\frac{\partial S}{\partial q_k} \right)^2 - U(\vec{q}, t) \quad (\text{HJE})$$

If we choose an initial condition for $S(\vec{q}, t)$ (which is equivalent to fixing the lower end point of the **AP** and choosing the initial velocities for every possible trajectory in the configuration space), together with the **GL**, the **HJE** allows the computation of all the possible trajectories at once. Contrary to the typical Newton's Second Law approach, where only a single trajectory is evolved (you chose an initial position and velocity), here, we compute all the trajectories (with initial velocities given by $S(\vec{q}, t = 0)$) at once! See how we have suddenly turned from trajectories into a wave guiding them.

Note now that the **(HJE)** is exactly the same as the **(QHJE)**, just that the QHJE has an additional potential term: the quantum potential **(Q)**. We could simply englobe **Q** in the general potential term, such that $U = V + Q$ would make both equations equal. Then, half of the **SE** is now understandable! Additionally, the wave S was obtained from trajectories in CM, so this coincidence very naturally suggests that we could introduce the concept of trajectory also in a quantum system (doing the opposite). Just consider **Q** as an additional potential term and the phase of the wave-function as the

¹Just knowing that space and time are homogeneous, space is isotropic, and assuming Galilean relativity -that the laws of physics are the same for any observer in a constant velocity with respect to an inertial frame- CM can be derived. Amazing!

Hamilton Principle Function S. Its variation in space, describes the velocity field that each possible “quantum trajectory” follows (**GL**). Well, this is what is called the set of **Bohmian Trajectories** [2] of a quantum system.

Let us now show how the **HJE** is equivalent to Newton’s Second Law. Take the **HJE** and repeat the following for each of the $k \in \{1 \dots n\}$: take the partial derivative with respect to q_k in both sides, apply Schwarz’s Theorem to exchange crossed partial derivatives on the first term of the *lhs* and do the derivative in the second. Then applying Schwarz’s theorem again for the terms in the summation to obtain:

$$\frac{\partial}{\partial t} \frac{\partial S(\vec{q}, t)}{\partial q_k} + \sum_{j=1}^n \frac{1}{m_j} \frac{\partial S(\vec{q}, t)}{\partial q_j} \frac{\partial}{\partial q_j} \frac{\partial S(\vec{q}, t)}{\partial q_k} = - \frac{\partial}{\partial q_k} U(\vec{q}, t)$$

Now, defining a system of discrete particles with trajectory $\vec{q}(t)$, the trajectory will follow the Guidance Law (**GL**), the S of which must satisfy the DE above. Evaluating the **GL** in the differential equation, we are left with:

$$\frac{\partial}{\partial t} \frac{\partial S(\vec{q}, t)}{\partial q_k} \Big|_{\vec{q}(t)} + \sum_{j=1}^n \frac{dq_j(t)}{dt} \frac{\partial}{\partial q_j} \frac{\partial S(\vec{q}, t)}{\partial q_k} \Big|_{\vec{q}(t)} = - \frac{\partial}{\partial q_k} U(\vec{q}, t) \Big|_{\vec{q}(t)}$$

Where we observe that the expression in the *lhs* is just the total time derivative of $\frac{\partial S(\vec{q}, t)}{\partial q_k}$ evaluated along the trajectory $\vec{q}(t)$. Thus, reverting the chain rule:

$$\frac{d}{dt} \frac{\partial S(\vec{q}, t)}{\partial q_k} \Big|_{\vec{q}(t)} = - \frac{\partial}{\partial q_k} U(\vec{q}, t) \Big|_{\vec{q}(t)}$$

Reverting the guidance law (**GL**) we get for each possible k the differential equation:

$$m_k \frac{d^2}{dt^2} q_k(t) = - \frac{\partial}{\partial q_k} U(\vec{q}, t) \Big|_{\vec{q}(t)} \quad \forall k \in \{1 \dots n\} \quad (\text{N2L})$$

which is *Newton’s Second Law*. The fun point is that all the development is valid as well for the **QHJE** ruling the **SE**. Therefore, there is a quantum version of (N2L): the *Bohmian Newton’s Law* (**BNL**). In principle it seems to allow the computation of independent trajectories like in CM. But we will see that in order to evolve a single trajectory we will need to compute all the rest of possible ones as well!

$$m_k \frac{d^2}{dt^2} q_k(t) = - \frac{\partial}{\partial q_k} [V(\vec{q}, t) + Q(\vec{q}, t)] \Big|_{\vec{q}(t)} \quad \forall k \in \{1 \dots n\} \quad (\text{BNL})$$

1.3 Then, what am I really computing when using the Schrödinger Equation?

In a nutshell, we first found that the Schrödinger Equation was nothing else but a convenient way to evolve two coupled *non-linear* DE-s (real ones) using a *single and linear* DE (a complex one). That is, solving the **SE** is exactly equivalent to simultaneously solving the **QHJE** and the **CE** for the quantum system.

Regarding the **QHJE** and the **HJE** of classical mechanics, we saw that apparently the only difference between the dynamics of a classical particle system and a Bohmian particle system is the presence of an additional Q potential term that appears always, independently of the typical potential V .

Now, we have so far skipped the other equation (**CE**), but it can easily be seen that it is an equation that forces a local continuity of the probability density, or equivalently of the ensemble of trajectories. Its derivation from scratch is shown in pg.23 of [3]. It is simply ensuring that there is no source or sink of $R^2 = |\psi|^2$, the probability density. Thus, it is the equation provoking the norm conservation of the wave-function. It is just about acknowledging that as well as a discrete trajectory $x(t)$ follows a velocity field $v(x, t)$ if it fulfills $\frac{dx(t)}{dt} = v(x, t)$, a continuous wave $\rho(x, t)$ follows the same velocity field if it fulfills the **CE**. So the mystery is not the equation but the role and relation of R^2 with the trajectories. We will see that R^2 can be interpreted as a continuity of particles, a current line of which turns out to be a possible Bohmian Trajectory. As such, the **CE** could also be seen as the equation that ensures an initial continuous distribution of infinite possible Bohmian Trajectories given by R^2 , follows the velocity field as an ensemble.

Then the keys we are left to show are, on the one hand, an intuitive understanding of what Q introduces to our apparent “particle” system and on the other hand, to see the role of the wave R^2 .

1.4 Why is it so hard to predict even just the motion of a single 1D particle?

The key lies in the way the two real equations are coupled: the **CE** forces the density R^2 to evolve according to the velocity field given by S , while the **QHJE** makes S evolve according to the *shape* of the density R^2 (which is what Q is) and the external potential.

Let us make Q intuitive. If we define the density $\rho(\vec{q}, t) := R^2(\vec{q}, t)$, we can see that the quantum potential can be restated as:

$$Q(\vec{q}, t) = - \sum_{k=1}^n \frac{\hbar^2}{2m_k R} \frac{\partial^2 R(\vec{q}, t)}{\partial q_k^2} = - \sum_{k=1}^n \frac{\hbar^2}{4m_k} \left(\frac{1}{\rho} \frac{\partial^2 \rho}{\partial q_k^2} - \frac{1}{2\rho^2} \left(\frac{\partial \rho}{\partial q_k} \right)^2 \right)$$

Defining the operator nabla $\nabla \equiv \left(\frac{\partial}{\partial q_1}, \dots, \frac{\partial}{\partial q_n} \right)$ we have:

$$Q(\vec{q}, t) = - \frac{\hbar^2}{4m_k} \left(\frac{\nabla^2 \rho}{\rho} - \frac{1}{2} \frac{(\nabla \rho)^2}{\rho^2} \right) \quad (\text{Q2})$$

According to the *Orthodox Interpretation* shown in most quantum mechanics text books, the system of quantum particles is a blur of possible outcomes that evolves unitarily as a wave until a measurement is realized, in which moment the whole wave-function non-locally collapses into a discrete particle, according to the probability density $\rho = R^2 = |\Psi|^2$. Instead, one could also interpret this observation using an apparently less mystical interpretation: the particle was always there. It was piloted by a velocity field due to S , and thus it should naturally have wave-like behaviour. But when observed, it turns out to be a particle, because it was always a particle². This would be the Bohmian Interpretation³. Sure, there is still the question of, what about the pilot wave S , is it ontologically as real as the particle? Is it just an aura surrounding any quantum system? Or rather a simple mathematical construct? In any case, it is still somewhat mystical in my opinion. In the last part of this section I offer an alternative personal interpretation to surpass these. But, for now we are well with these two well established interpretations to understand Q .

Accepting that before the collapse of the wave-function, the system was already an ontologically discrete trajectory or not, it is clear from the empirical point that $\rho(\vec{q}, t)$ describes the probability to find the particle at a certain point. We can imagine it as giving the density of possible experimental outcomes if a measurement was realized in each time (the *Orthodox*), or rather as a density of possible trajectories of the particles that actually are ontologically concrete at all times (Bohmian), it does not matter.

The first term in Q is the Laplacian ($\nabla^2 = \frac{\partial^2}{\partial q_1^2} + \dots + \frac{\partial^2}{\partial q_n^2}$) of $\rho(\vec{q}, t)$ in each point, normalized by the value of ρ in that point. The Laplacian of a scalar field in a certain point gives the difference between the value of the function in that point and the mean value in its locality (see **Appendix D**). Interpreting this value as a potential, means that the higher the local variation of ρ (the higher the difference between the value in the point and its mean value in the surrounding), the bigger the modulus of the potential will be. In particular, if the Laplacian of ρ is positive, it means that the value in the point is smaller than the mean surrounding density, that is, the density is more convex-like there. This makes the potential at that point be negative-attractive- (noting the minus sign in front of the Laplacian). The particle will be more stable there than in points where the variation of the density is more concave-like (where the value of the density is higher than in its local surrounding: $\nabla^2 \rho < 0$), as these make a positive-repulsive- contribution to the total potential in their locality.

Interpreting ρ as the density of all the possible observations, this means that the possibility of presence of particle (and thus their density⁴) are repelled by the points where there is a high agglomeration of probability for the particle's presence.

²As it is wisely stated in Ref.[1], one thing cannot be both a particle and a wave at the same time, but two can: the particle and the guiding pilot wave S

³Which is perfectly equivalent to the Orthodox Formalism. Actually Bohm himself developed a framework for the measurement which does not involve any kind of collapse [5][6] (even if it is still probabilistic and non-local).

⁴ The density R^2 and the particles are evolved using the same velocity field

The second term in Q is more straight-forward: it is the modulus of the gradient of the density in each point normalized by the magnitude of the density. The fraction is always a positive value, which means the contribution to the potential will always be positive: it is a destabilizing factor (repels trajectories). That is, the higher the local steepness of the density, the more unstable this zone will be for the particle.

We can now intuitively understand why a quantum free particle, given by a Gaussian packet with no initial momentum in null potential $V = 0$ tends to open and broaden (Figure 1). Even if there is no kinetic energy and no external potential, there is motion because the non homogeneous agglomeration of probability density (or Bohmian trajectories), produces a quantum potential Q that is shaped actually like an inverse parabolla [7][1]. The possible Bohmian trajectories repel each other, so they tend to get as homogeneously distributed as possible (the same goes for probability density). So the Gaussian packet will broaden forever until in $t \rightarrow \infty$ an homogeneity of ρ is achieved (as $Q \rightarrow 0$).

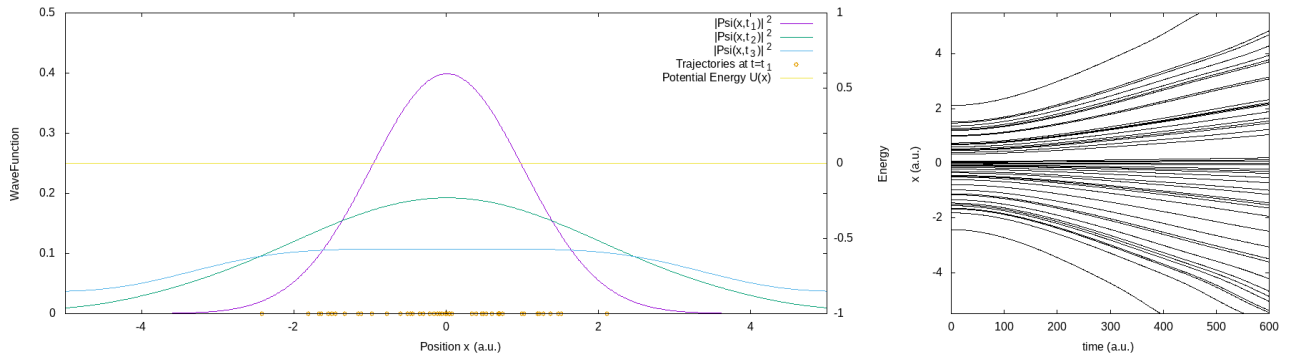


Figure 1: Time evolution using the Crank-Nicolson algorithm, of a gaussian 1D wave-packet in free space $V(x, t) = 0$. On the left, three different time snapshots of the probability density. The yellow dots on the x axis represent the initial positions of several Bohmian Trajectories. The time evolution of the trajectories is shown on the right. In atomic units.

Then, what should we do to stop that broadening? Well, if the total potential field is $U = V + Q$ and the curvature of the Gaussian causes $Q \propto -x^2$ an inverted parabola, then we will need to set $V(x) \propto +x^2$. Wait, we have just found why the ground state of a harmonic well $V(x) = ax^2$ happens to be a Gaussian! In essence, we can now understand as well why a displaced Gaussian in a harmonic well oscillates back and forth around the minimum, but the centered one (with the correct parameters to cancel the quantum potential Q) remains still. Actually, this analysis can be extended to understand the particular shapes of any stationary state of any potential $V(x)$. They are the special shapes the ensemble of trajectories or the probability density must take, in order for the discomfort the trajectories feel due to them being agglomerated be harmonized with the stable points of the external potentials. There is where the trajectories will be in comfort. The second and third stationary states of the harmonic well are alternative particular shapes that also happen to cancel the “agglomeration discomfort” (see Fig 2). That’s why they are stationary sates of this system.

Actually, we can now understand why the wave-function in a harmonic well does not collapse into the potential minimum in a sort of Dirac-Delta (which is what our classical intuition would tell us from an ensemble of classical particles in a well). It is because, sure, most of the trajectories will tend towards the minimum, but a certain agglomeration will arrive in each vicinity of the minimum, that will make the minimum undesirable (due to the internal quantum pressure). It is as if the agglomerated probability density avoided the rest to go closer to the minimum. That is, the most central trajectories are so congregated that the repulsive force they feel with one another makes them suspend the rest of the trajectories at non null potential energies. Something that would classically be unthinkable. But if we think for a moment, classically there is no principle or general force that makes bodies not want to superimpose. It seems like we have found a fundamental force that avoids particle congregation...or have we?

Everything stated till now is fully compatible with experimental observations. Now, there is a very subtle point, which made me see the need of another interpretation: we are understanding that

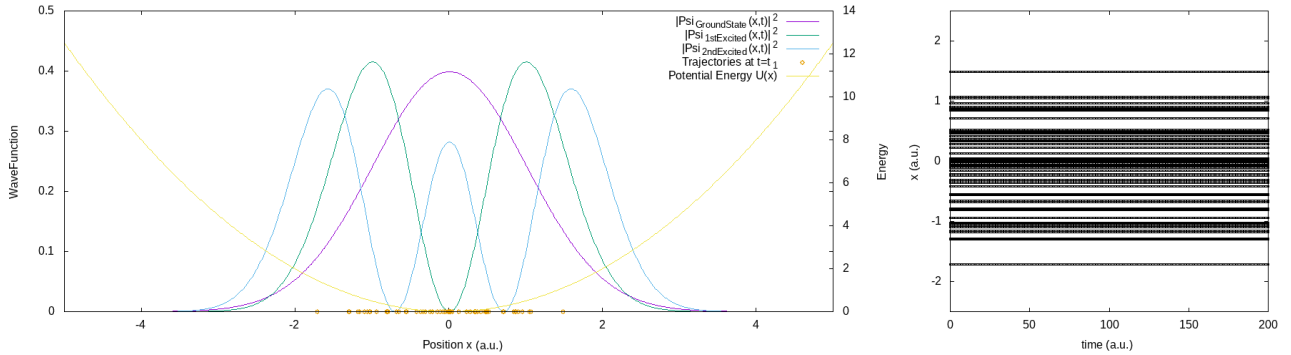


Figure 2: Time evolution using the Cranck-Nicolson algorithm, of a Gaussian 1D wave-packet in a harmonic well $V(x,t) = 0.5x^2$ (in atomic units $\hbar = 1$, $m = 1$). On the left, the first three stationary states' probability densities. The yellow dots on the x axis represent the initial positions of several Bohmian Trajectories. The time evolution the trajectories is shown in the right (stationary, as expected).

there is a sort of repulsive pairwise interaction among every two Bohmian trajectories (every two possible experimental outcomes), that for instance allows a quantum particle be hanging, stationary, in a non minimum potential energy point. But now notice, that we are not talking about separate different particles, but about possible different experimental observations of a same particle! So we are literally acknowledging that trajectories that could have been, but are not real, affect contingently the trajectory we observe. That is, there is a dynamical, contingent influence of all the possible experimental outcomes on the one you finally see. Be an Orthodox or a Bohmian, but you will not find any explanation. A single quantum experiment physically contains the information of the rest of possible outcomes! We will come to this again.

Let us enlighten the many body problem in an alternative way. We have an exact Quantum Newton like expression (**BNL**). But why can't we compute just a single trajectory given an initial point and velocity like in CM? Because the computation of Q explicitly depends on how the density of possible trajectories R^2 is shaped! That is, you need to compute the whole R at each time in order to have the information of the forces on a single trajectory. While in classical mechanics, using the **HJE** and evolving every possible trajectory at once was an option, in QM, it is not an option. You need them to describe Q !. Nature has doomed us to compute all the possible experimental outcomes in order to predict only one of them. Be an Orthodox or not this analogy is strictly true in computational means. That is, if I want to simulate the evolution of a quantum system, I am forced to simulate every single possible trajectory. So, imagine how must the complexity of possible trajectories grow with increasing spatial dimensions! Each dimension you add to the simulation, would curse you to compute your previous grid times the points you consider in the new coordinate! This scales absurdly. And this is, the curse of the many bodies in QM.

1.5 The Literal Interpretation of Quantum Mechanics : An existential relief?

What follows is the begging of a new interpretation of QM I am working in on a separate dissertation, so if you are already comfortable with the *non-sense intuition wholes* I mentioned, you can jump to the next section and may you be praised.

Most of the readers will have already seen where I am trying to go. More than the description of possible trajectories for one particle or a probability density for one particle (Bohmian or Orthodox), ρ seems to match more clearly the behaviour of a fluid![8] If one was to literally interpret the mathematics of quantum mechanics, it would seem very natural to understand ρ as a continuity of particles, a fluid. Not just all the **possible** realities of the observed particle, but an actual infinite ensemble of particles, the trajectories of which, affect mutually in a perceivable way. Each of the spatial dimensions of ρ seems to represent the limit of infinite adjacent particles (the observed Bohmian particle, would just be one of these). The rest of unobserved particles, simply make a pressure on this observed particle (as they exert among them as well) and drive it according to the typical behavior of a continuous matter *wave* where particles cannot cross each other and actually repel high concen-

trations of them. Everything seems to match with this view: The non crossability of the trajectories is straightforward from the Theorem of Existence and Uniqueness of initial value solutions to ODEs. The fact that they influence repulsively is encoded, as we explained, in the potential Q . Everything matches in the maths, until you go and observe the system, and suddenly there is only one discrete particle of all the points in the fluid!

I agree with the Orthodox criticism to Bohmian Interpretations: the particle concept is an *add on* in the SE, in the maths of QM: it is only due to the observation of a single particle that we feel comfortable introducing it. But if one did not attend to the observed discrete particle, the mathematics of QM clearly show a continuous distribution of particles in each dimension. Make this wave of particles more compact, and they will tend to repel each other more strongly. There is an internal quantum pressure Q , while V simply describes geometrical constraints between the degrees of freedom.

But then, why do we only observe one of the possible trajectories in the fluid? My answer is very straight-forward: trajectories cannot cross each other in the configuration space. Let me explain. Which is the most general and theoretically the only valid wave-function, capturing all the entanglements etc? Well, the wave-function of all the particles in the Universe. Then, one trajectory of the fluid that this ensemble of parallel trajectories implies, would be a discrete observation of the whole Universe (every particle at a certain location). This Universal world-line **is** affected by the rest of possible trajectories contingently, hence, the information of the rest of “particles” **IS** in the reality. Which literally interpreting it, would mean that those other possible Universal trajectories that affect ours, actually **are** as contingent as ours. Then, why don’t we observe them? Well, trajectories cannot cross in the configuration space⁵. We, as observers, only experience one trajectory, we experience a single Universe, and we are doomed in this trajectory forever.

I like to call this the **Tangent** Universe Interpretation, because, the rest of possible trajectories, are not just *parallel*, like a trajectory of the same particle with a different initial position would be in Newtonian dynamics with respect to the first, instead, they influence each other, expressing discomfort when they are agglomerated, and bending the actual trajectory taken by the observed particle. Somehow, the presence of the rest of Universes can be felt “tangentially”, like when the particle in the double slit appears to be pushed by the rest of “possible” outcomes.

This interpretation is pleasant to intuition because it seems to resolve many of the misconceptions of QM: it does not break realism and is ontologically deterministic, the reason why we do not observe “quantum superpositions” at large scales is clear (we only experience a single trajectory), the reason why the outcome of a quantum experiment is probabilistic is somewhat clear as well (not every trajectory can occupy a same state, thus there is an unavoidable dispersion around the potential minima: we will happen to be in one of those possible alternative trajectories pondered by their “relative amount” R^2). We could even try to check if non-locality could be understood as well as a natural consequence of the propagation of a pressure wave across the fluid that could be faster than light.

Physicists among the readers must be hissing by now, but let me tell you that if I need to compute all the possible trajectories of a system in order to predict the behavior of the wavefunction, then, **in** the reality as well, the way an electron is driven in a slit diffraction encodes the influence of all the possible trajectories. That is, physically the information exists, a contingent influence of the rest of particles exists (a force if you prefer, check in [BNL](#) that $\frac{\partial Q}{\partial q_k}$ acts just like a common generalized force in Newton’s Laws: but its magnitude and sign are influenced by the shape of the ensemble of “possible” trajectories). How to make this intuitive other wise? Possibly I am wrong, but don’t we consider, whenever there is an external contingent influence/force on a system, that it is due to something that must contingently exist? Like when we talk about the presence of an electric field, or a magnetic field, or a gravitational wave. All of them influence the motion of bodies in the Universe, and sure, we could neglect the existence of a source for them. But as their effect is so contingent, we tend to accept (and can even predict) the particle that produced such an effect. Because the information of its existence and properties are engraved in their influence. Well, why do we then look the other way when it comes to the quantum pressure?

⁵Due to the Theorem of Existence and Uniqueness of solutions to initial value ODEs

2 Trying to achieve the exactest numerical time evolution: the Cranck-Nicolson algorithm

Let us now present an algorithm that allows a numerical time evolution using the exact **SE**. We will prove that it is unfeasible for problems concerning more than a few degrees of freedom, as a clear practical manifestation of the many body problem that we theoretically found in the previous section.

Given the Hamiltonian Operator of the n degree of freedom Schrödinger Equation (**SE**):

$$\hat{H} = - \sum_{k=1}^n \frac{\hbar^2}{2m_k} \frac{\partial^2}{\partial q_k^2} + V(q_1, \dots, q_n, t)$$

We have that the **SE** can be rewritten as:

$$\frac{\partial \psi(\vec{q}, t)}{\partial t} = \frac{-i}{\hbar} \hat{H} \psi(\vec{q}, t)$$

Which means that given an initial state for the wavefunction at t_0 : $\psi(\vec{q}, t = t_0) = \rho(\vec{q}, t_0) e^{iS(\vec{q}, t_0)/\hbar}$, the state-vector of the system in the subsequent times will be:

$$\psi(\vec{q}, t) = e^{-\frac{i}{\hbar} \int_{t_0}^t \hat{H} dt} \psi(\vec{q}, t = t_0)$$

We define the propagator operator as:

$$\hat{U}(t) := e^{-\frac{i}{\hbar} \int_{t_0}^t \hat{H} dt} \quad (\text{PO})$$

This operator will input the wavefunction at t_0 and output it at any t . Now, the point is that if we discretize time, we will only be interested on the wavefunction on the time instances of the grid. Therefore, we will have enough with an operator to jump from time to time. If we assume that the time step Δt is small enough, even if the Hamiltonian depends on time, the discrete propagator operator form time t_0 to $t_0 + \Delta t$ with $\Delta t \rightarrow 0$ will be:

$$\hat{U}(t = t_0 + \Delta t) \simeq e^{-\frac{i\hat{H}(t_0)}{\hbar} (\Delta t)} = e^{-\frac{i\hat{H}(t_0)}{\hbar} \Delta t}$$

Note that if the Hamiltonian did not depend on time, the operator obtained this way would be useful for any time and the relation would be an equality. Else, we would have to redefine the operator in each time iteration, and would only hold reasonably true if the variation time scale of $\hat{H}(t)$ is way slower than the considered Δt .

\hat{U} is a unitary operator ($\hat{U}^\dagger \hat{U} = \hat{I}d = \mathbf{1}$), which means that it will preserve the norm of the wavefunction at all times ($|\psi(\vec{q}, t = t_0)|^2 = |\psi(\vec{q}, t)|^2 \quad \forall t$). In turn, any approximation of the propagator operator will be required to be unitary. That is why we could not simply use:

$$\hat{U}(t_0 + \Delta t) \simeq 1 - \frac{i\hat{H}\Delta t}{\hbar} + o(\Delta t^2)$$

Instead, we could split $\hat{U}(t_0 + \Delta t)$ as follows:

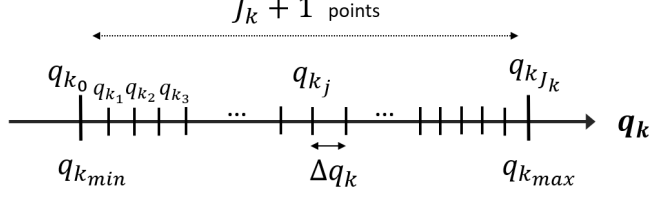
$$\hat{U}(t_0 + \Delta t) = e^{-\frac{i\hat{H}\Delta t}{2}} e^{-\frac{i\hat{H}\Delta t}{2}} = \frac{e^{-\frac{i\hat{H}\Delta t}{2}}}{e^{\frac{i\hat{H}\Delta t}{2}}} \simeq \frac{1 - \frac{i\hat{H}\Delta t}{2\hbar}}{1 + \frac{i\hat{H}\Delta t}{2\hbar}} + o(\Delta t^2)$$

which is now unitary. This is called the **Cayley Form** of the operator[9]. Rearranging, this leaves us the following numerical approximation of the Schrödinger time evolution:

$$\left(1 + \frac{i\Delta t}{2\hbar} \hat{H}\right) \psi(\vec{q}, t + \Delta t) = \left(1 - \frac{i\Delta t}{2\hbar} \hat{H}\right) \psi(\vec{q}, t) \quad (\text{AproxSE})$$

$$\left(1 + \frac{i\Delta t}{2\hbar} \left(- \sum_{k=1}^n \frac{\hbar^2}{2m_k} \frac{\partial^2}{\partial q_k^2} + V(\vec{q}, t + \Delta t) \right) \right) \psi(\vec{q}, t + \Delta t) = \left(1 - \frac{i\Delta t}{2\hbar} \left(- \sum_{k=1}^n \frac{\hbar^2}{2m_k} \frac{\partial^2}{\partial q_k^2} + V(\vec{q}, t) \right) \right) \psi(\vec{q}, t)$$

Let us introduce an equi-spaced discretization into the spatial degrees of freedom $\{q_1, \dots, q_n\}$. We will denote the number of discrete spatial intervals for each of the n dimensions as $\{J_{q_1}, \dots, J_{q_n}\}$. Each discrete spatial point will be $q_{k_j} := q_{k_{min}} + j\Delta q_k$ with $j \in \{0, 1, 2, \dots, J_{q_k}\}$ and $k \in \{1 \dots n\}$. Where we defined the step in the k -th spatial dimension as $\Delta q_k := (q_{k_{max}} - q_{k_{min}})/J_{q_k}$. $q_{k_{max}}$ and $q_{k_{min}}$ denote the two endpoints of the considered total interval of the grid in each dimension.



For a shorter notation we will just write the wave-function as a function of the grid point indices. Also, we will tag it with *prev* when then time is t , *next* if time is $t + \Delta t$ and *curr* if undefined. E.g.:

$$\psi_{(j_1, j_2, \dots, j_n)}^{next} := \psi(q_{1,j_1}, q_{2,j_2} \dots q_{n,j_n}, t + \Delta t)$$

$$\psi_{(j_1+1, j_2-1, j_3, \dots, j_n)}^{prev} := \psi(q_{1,j_0} + \Delta q_1, q_{2,j_2} - \Delta q_2, q_{3,j_3}, \dots q_{n,j_n}, t)$$

For the spatial partial derivatives we will use a second order central finite difference:

$$\frac{\partial^2}{\partial q_k^2} \psi(q_1, \dots, q_n, t) = \frac{\psi(q_1, \dots, q_k + \Delta q_k, \dots, q_n, t) - 2\psi(q_1, \dots, q_k, \dots, q_n, t) + \psi(q_1, \dots, q_k - \Delta q_k, \dots, q_n, t)}{(\Delta q_k)^2} + o((\Delta q_k)^2)$$

which using the notation introduced above reads:

$$\frac{\partial^2}{\partial q_k^2} \psi_{(j_1, \dots, j_k, \dots, j_n)}^{curr} = \frac{\psi_{(j_1, \dots, j_k+1, \dots, j_n)}^{curr} - 2\psi_{(j_1, \dots, j_k, \dots, j_n)}^{curr} + \psi_{(j_1, \dots, j_k-1, \dots, j_n)}^{curr}}{(\Delta q_k)^2} + o((\Delta q_k)^2)$$

Introducing the central differences and the discretization to equation (AproxSE), we get the basic equation for the Cranck Nicolson Method for an arbitrary number of spatial degrees of freedom:

$$\begin{aligned} \psi_{(j_1, \dots, j_n)}^{next} - \frac{i\Delta t}{2\hbar} \left[\sum_{k=1}^n \frac{\hbar^2}{2m_k} \left(\frac{\psi_{(j_1, \dots, j_k+1, \dots, j_n)}^{next} - 2\psi_{(j_1, \dots, j_k, \dots, j_n)}^{next} + \psi_{(j_1, \dots, j_k-1, \dots, j_n)}^{next}}{(\Delta q_k)^2} \right) - V_{j_1, \dots, j_k}^{next} \psi_{(j_1, \dots, j_n)}^{next} \right] = \\ = \psi_{(j_1, \dots, j_n)}^{prev} + \frac{i\Delta t}{2\hbar} \left[\sum_{k=1}^n \frac{\hbar^2}{2m_k} \left(\frac{\psi_{(j_1, \dots, j_k+1, \dots, j_n)}^{prev} - 2\psi_{(j_1, \dots, j_k, \dots, j_n)}^{prev} + \psi_{(j_1, \dots, j_k-1, \dots, j_n)}^{prev}}{(\Delta q_k)^2} \right) - V_{j_1, \dots, j_k}^{prev} \psi_{(j_1, \dots, j_n)}^{prev} \right] \end{aligned}$$

Grouping up terms we get the master equation of the Cranck-Nicolson method:

$$\begin{aligned} b_{(j_1, \dots, j_n)}^{next} \psi_{(j_1, \dots, j_n)}^{next} + \sum_{k=1}^n a_k \left(\psi_{(j_1, \dots, j_k-1, \dots, j_n)}^{next} + \psi_{(j_1, \dots, j_k+1, \dots, j_n)}^{next} \right) = \\ = d_{(j_1, \dots, j_n)}^{prev} \psi_{(j_1, \dots, j_n)}^{prev} - \sum_{k=1}^n a_k \left(\psi_{(j_1, \dots, j_k-1, \dots, j_n)}^{prev} + \psi_{(j_1, \dots, j_k+1, \dots, j_n)}^{prev} \right) \end{aligned} \quad (\text{CN})$$

where, coefficients b and d depend on the spatial grid position and the time iteration, while a_k is constant for any spatial or time point and just depends on k :

$$b_{(j_1, \dots, j_n)}^{next} = 1 + \frac{i\Delta t \hbar}{2} \sum_{k=1}^n \left(\frac{1}{m_k (\Delta q_k)^2} \right) + \frac{i\Delta t}{2\hbar} V_{(j_1, \dots, j_n)}^{next}$$

$$d_{(j_1, \dots, j_n)}^{next} = 1 - \frac{i\Delta t \hbar}{2} \sum_{k=1}^n \left(\frac{1}{m_k (\Delta q_k)^2} \right) - \frac{i\Delta t}{2\hbar} V_{(j_1, \dots, j_n)}^{next}$$

$$a_k = -\frac{i\Delta t \hbar}{4m_k (\Delta q_k)^2}$$

Observe how b is actually the complex conjugate of d . Aka, $b_{(j_1, \dots, j_n)}^{cur} = \overline{d_{(j_1, \dots, j_n)}^{cur}}$.

This last shape of the numerical SE, will allow us to express the time evolution in a very convenient matrix equation. Computationally transforming problems into algebraic matrix problems is very convenient, as tons of methods for linear algebra have already been optimized.

It would seem natural to store the $n + 1$ dimensional discretized wave-vector at each time, as an n dimensional tensor. The point is that as the memory of a computer is sequential, the tensor will internally end up being saved as a planed linear vector. Noting this and the fact that matrix (2-tensor) and vector (1-tensor) algebras are computationally easier to treat, we will start by lining up the n -tensor ourselves. That is, for each time, we will save the discretized n dimensional wave-function as a vector, following the transformation:

$$\vec{\psi}^{cur} = \left(\psi_{(0,0,0\dots 0)}^{cur}, \dots, \psi_{(J_{q1},0,0\dots 0)}^{cur}, \psi_{(0,1,0\dots 0)}^{cur}, \dots, \psi_{(J_{q1},1,0\dots 0)}^{current}, \dots, \psi_{(J_{q1},J_{q2},0\dots 0)}^{cur}, \dots, \psi_{(J_{q1},\dots,J_{qn})}^{cur} \right) \in \mathbb{C}^{(J_{q1}+1)\dots(J_{qn}+1)}$$

Ultimately, we will get a matrix equation of the form:

$$U_L \vec{\psi}^{next} = U_R \vec{\psi}^{prev}$$

with $U_L, U_R \in \mathcal{M}_{(J_{q1}+1)\dots(J_{qn}+1) \times (J_{q1}+1)\dots(J_{qn}+1)}(\mathbb{C})$ giant but luckily sparse complex matrices with only $2n + 1$ non-zero elements per column and such that $U_L = \overline{U_R}$. Let us now develop the shape of these matrices. We will obtain them inductively, by first considering the $n = 1$ case, then the $n = 2$ case, then $n = 3$ and finally generalizing it to $n = N$ dimensions.

2.1 n=1: One spatial dimension

In this simple case of one quantum particle restricted to one dimension, we will have that the discretized wave-vector at each time will indeed be a vector $\vec{\psi}^{curr} = (\psi_0^{curr}, \dots, \psi_J^{curr}) \in \mathbb{C}^{J+1}$, with the j -th element of the vector being:

$$\psi_j^{next} := \psi(q_j, t + \Delta t) = \psi\left(q_{min} + j \frac{(q_{max} - q_{min})}{J}, t + \Delta t\right) \text{ with } j \in \{1, 2, \dots, J\}$$

The time evolution will need to follow the $n = 1$ case of equation **CN**:

$$b_j^{next} \psi_j^{next} + a(\psi_{j-1}^{next} + \psi_{j+1}^{next}) = d_j^{prev} \psi_j^{prev} + a(\psi_{j-1}^{prev} + \psi_{j+1}^{prev})$$

where:

$$b_j^{next} = 1 + \frac{i\Delta t \hbar}{2m(\Delta q)^2} + \frac{i\Delta t}{2\hbar} V_j^{next}; \quad d_j^{next} = 1 - \frac{i\Delta t \hbar}{2m(\Delta q)^2} - \frac{i\Delta t}{2\hbar} V_j^{next}$$

$$a = \frac{-i\Delta t \hbar}{4m(\Delta q)^2}$$

Which can conveniently be arranged into the following matrix equation:

$$U_L \vec{\psi}^{next} = U_R \vec{\psi}^{prev}$$

With U_L and U_R complex conjugate $(J + 1) \times (J + 1)$ tridiagonal matrices:

$$U_L = \begin{pmatrix} b_0 & a & & & \\ a & b_1 & a & & \\ & a & b_2 & a & \\ & & \ddots & \ddots & \ddots \\ & & & a & b_{J-1} & a \\ & & & & a & b_J \end{pmatrix}; \quad U_R = \begin{pmatrix} d_0 & -a & & & \\ -a & d_1 & -a & & \\ & -a & d_2 & -a & \\ & & \ddots & \ddots & \ddots \\ & & & -a & d_{J-1} & -a \\ & & & & -a & d_J \end{pmatrix}$$

$$U_L = \overline{U_R}$$

2.2 n=2: Two spatial dimensions (2 quantum 1D particles or a single 2D particle)

This time, the discretized state at a certain time ψ^{cur} should be represented as a matrix, but following the discussion in the general case, we will encode it in a sequential vector:

$$\vec{\psi}^{curr} = (\psi_{00}^{curr}, \psi_{10}^{curr}, \dots, \psi_{J_1 0}^{curr}, \psi_{01}^{curr}, \psi_{11}^{curr}, \dots, \psi_{J_1 J_2}^{curr}) \in \mathbb{C}^{(J_1+1) \times (J_2+1)}$$

such that:

$$\psi_{jk}^{next} := \psi(q_{1j}, q_{2k}, t + \Delta t) = \psi\left(q_{1min} + j \frac{(q_{1max} - q_{1min})}{J_1}, q_{2min} + k \frac{(q_{2max} - q_{2min})}{J_2}, t + \Delta t\right)$$

The time evolution will need to follow the $n=2$ case of equation CN:

$$b_{jk}^{next} \psi_{jk}^{next} + a_1(\psi_{j-1,k}^{next} + \psi_{j+1,k}^{next}) + a_2(\psi_{j,k-1}^{next} + \psi_{j,k+1}^{next}) = \\ = d_{jk}^{prev} \psi_{jk}^{prev} + a_1(\psi_{j-1,k}^{prev} + \psi_{j+1,k}^{prev}) + a_2(\psi_{j,k-1}^{prev} + \psi_{j,k+1}^{prev})$$

where:

$$b_{jk}^{next} = 1 + \frac{i\Delta t \hbar}{2} \left(\frac{1}{m_1(\Delta q_1)^2} + m_2(\Delta q_2)^2 \right) + \frac{i\Delta t}{2\hbar} V_{jk}^{next}$$

$$d_{jk}^{next} = 1 - \frac{i\Delta t \hbar}{2} \left(\frac{1}{m_1(\Delta q_1)^2} + m_2(\Delta q_2)^2 \right) - \frac{i\Delta t}{2\hbar} V_{jk}^{next}$$

$$a_r = \frac{-i\Delta t \hbar}{4m_r(\Delta q_r)^2}$$

Arranged into a matrix equation:

$$U_L \vec{\psi}^{next} = U_R \vec{\psi}^{prev}$$

with U_L and U_R complex conjugate $(J_1 + 1)(J_2 + 1) \times (J_1 + 1)(J_2 + 1)$ sparse matrices with at most 5 non-null elements per column:

$$U_L = \left(\begin{array}{cc|cc|c} b_{00} & a_1 & a_2 & & \\ a_1 & b_{10} & a_1 & a_2 & \\ \ddots & \ddots & \ddots & \ddots & \\ a & b_{J_1,0} & & a_2 & \\ \hline a_2 & & b_{01} & a_1 & a_2 \\ & a_2 & a_1 & b_{11} & a_1 & a_2 \\ & & \ddots & \ddots & \ddots & \ddots \\ & a_2 & & a_1 & b_{J_1,1} & a_2 \\ & & a_2 & & \bullet & a_2 \\ & & & a_2 & \bullet & a_2 \\ & & & \ddots & \bullet & \ddots \\ & a_2 & & a_2 & & a_2 \\ & & a_2 & & \bullet & a_2 \\ & & & a_2 & & a_2 \\ & & & & a_2 & b_{0J_2} \\ & & & & a_1 & b_{0J_2} & a_1 \\ & & & & \ddots & \ddots & \ddots \\ & & & & a_2 & & a_1 & b_{1J_2} \end{array} \right); \quad U_R = \overline{U_L}$$

Where it can be noted that the matrix contains the same U_L matrix we had in the 1D case but replicated for each of the possible positions in the second dimension ($J_2 + 1$ times). Therefore, we see that the increase in dimension makes the matrix much larger.

2.3 n=3 and n=N: Generalization of the CN matrix approach

$n = 3$ could be seen as the example of a single particle in our physical world, that is, a quantum particle in 3D. This time, the discretized state at a certain time should be represented as a 3-tensor (3D matrix), but following the discussion above, we will encode it in a (quite big) sequential vector:

$$\vec{\psi}^{curr} = (\psi_{000}^{curr}, \dots, \psi_{J_1 00}^{curr}, \psi_{010}^{curr}, \dots, \psi_{J_1 10}^{curr}, \dots, \psi_{J_1 J_2 0}^{curr}, \psi_{001}^{curr}, \dots, \psi_{J_1 J_2 1}^{curr}, \dots, \psi_{J_1 J_2 J_3}^{curr}) \in \mathbb{C}^{(J_1+1) \times (J_2+1) \times (J_3+1)}$$

The time evolution would need to follow the $n=3$ case of equation CN. Arranged into a matrix equation like: $U_L \vec{\psi}^{next} = U_R \vec{\psi}^{prev}$, we would have U_L and U_R are complex conjugate $(J_1 + 1)(J_2 + 1)(J_3 + 1) \times (J_1 + 1)(J_2 + 1)(J_3 + 1)$ sparse matrices with at most 7 non-null elements per column. Drawing the whole matrix in a page is difficult, but following the idea we observed for the $n=2$ case its pattern can easily be understood. U_L will contain in its diagonal a “repetition” of the 2D U_L , repeated $(J_3 + 1)$ times with two bands of a_3 coefficients crossing the diagonals that touch the vertices of the copies of 2D U_L -s, just like the a_2 did with the vertexes of the 1D sub-matrix blocks. See the third matrix in Figure 3.

We are now ready to intuitively generalize the shape of the propagator matrices U_L and U_R to arbitrary N dimensions ($n = N$). Noting this sort of fractal construction: per each additional dimension $n = k + 1$, we can take the U_L and U_R of the previous case $n = k$ and repeat it as many times as points we consider in the new dimension ($J_{q_k} + 1$). For each repetition, we set a different index for the new dimension, and put them as diagonal blocks of a bigger matrix. Each of these blocks will describe the time evolution of all the rest of dimensions conditioned to a particular point of the newly considered one. Additionally, we will set the a_{k+1} coefficients repeated diagonally tangent to the edges of the blocks of one less dimension.

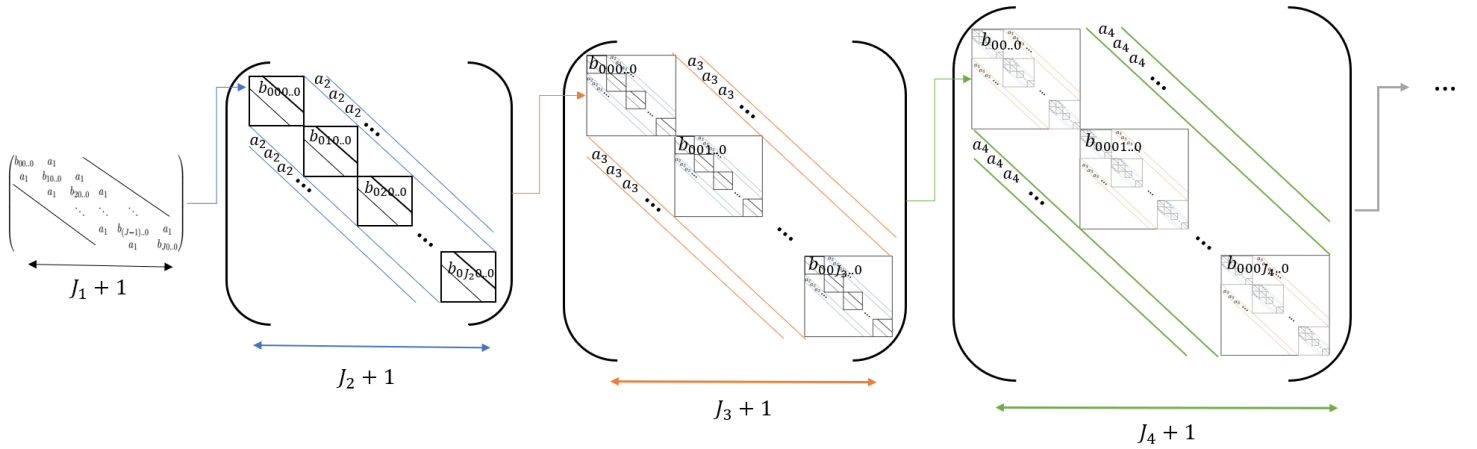


Figure 3: Schematic representation of the “fractal” construction of U_L for several dimensions. Then $U_R = \overline{U_L}$

Beginning the induction in the $n = 1$ case we described (follow Figure 3), we build a tridiagonal matrix with $J_1 + 1$ terms in the main diagonal (one for each position in q_1). We repeat this whole matrix $J_2 + 1$ times as diagonal blocks of a larger matrix (once per each position in $q_2 : J_2 + 1$ times). At the same time, all this construction will be repeated as diagonal blocks of an even bigger matrix where it will be repeated for each position in q_3 ($J_2 + 1$). This whole monster sparse matrix will now be fractally repeated as sub-matrix blocks of a bigger matrix as many times as points in q_4 ($J_2 + 1$), and so on iteratively until q_n . Do not forget about the a_k coefficient bands in each step!

We have somewhat algorithmically shown here how even **spatially**, the problem of more quantum bodies increases exponentially in complexity. Let us now prove that also **temporally** (in computation time), the problem grows exponentially.

2.4 How to solve the matrix equation?

Once we have created the numerical framework to evolve the wavefunction, we will now need to choose the way we solve the matrix equation $U_L \vec{\psi}^{next} = U_R \vec{\psi}^{prev}$, such that given U_L , U_R , $\vec{\psi}^{prev}$ we seek to find $\vec{\psi}^{next}$. An obvious way would be to invert U_L and generate a propagator matrix $U_L^{-1}U_R$ s.t $\vec{\psi}^{next} = U_L^{-1}U_R \vec{\psi}^{prev}$. The point is that the direct numerical obtention of an inverse matrix is numerically unpleasant. Instead, we will cast the problem into a linear equation system solving of type $A\vec{x} = \vec{b}$ where $\vec{b} = U_R \vec{\psi}^{prev} \in \mathbb{C}^{(J_{q_1}+1)\cdots(J_{q_n}+1)}$ and $A = U_L \in \mathcal{M}(\mathbb{C})^{(J_{q_1}+1)\cdots(J_{q_n}+1) \times (J_{q_1}+1)\cdots(J_{q_n}+1)}$ are a known vector and matrix at each time. We are looking for the vector $\vec{x} = \vec{\psi}^{next}$. To solve this system, *LU Decomposition* methods are very convenient as explained in any numerical method text book. See pg. 152 in Ref [10] for instance. In this reference, one can additionally see the proof that

the computational complexity of solving an equation system this way is $O(\frac{2}{3}m^3)$ for a dense general $m \times m$ matrix. In our case we have sparse matrices with only $2n + 1$ non-zero entries per column (n is the number of dimensions of the quantum system). Such sparcities allow faster algorithms, like the one reported in Ref [11], where it is found that a LU factorization can be performed in $O(m^{3/2})$. But even if there was an algorithm that allowed to solve our equation system as fast as $O(n \cdot m)$ (manipulating less than once each entry of the sparse matrices, which is a very generous lower bound), we will see the problem scales absurdly. m is the number of columns in U_L and U_R , which we said was $(J_{q_1} + 1) \cdots (J_{q_n} + 1)$, with J_{q_k} the number of divisions in the grid for the $k - th$ dimension. In general, we will seek to have an equilibrated grid, where every dimension has a number of divisions of the same order of magnitude, let us call this number J . Then the matrix has $m \sim J^n$ columns (J times more for each dimension in the quantum system). Thus, for the idyllically fast $O(n \cdot m)$ algorithm, each decomposition will need more than nJ^n computer operations, which as n grows, becomes exponentially more time consuming. In particular, if we want to perform on the order of J time iterations, then the bound for the complexity is $O(nJ^{n+1})$. Which is absurdly big!

Let us put some example numbers. Assuming a poorly defined spatial grid $J \sim 100$, at a big 0.01 time step and a CPU time per operation of an idyllic 1ns/op : we can see in Table 1 that for the time evolution of a *single* H_2 molecule in physical space (3D), which has $4 * 3$ degrees of freedom ($2 e^-$, $2 p^+$), we would require a computation time several times the current estimated age of the Universe (the Andromeda Galaxy and the Milky Way will have already collided long ago, so yeah, we will definitely not be there)!

Such is the magnitude of the Quantum Many Body *Curse*. Clearly we cannot pretend to solve the SE as exactly as possible. Hence, the necessity of approximations is now crystal clear.

Table 1: The time complexity scaling using an unreal idyllic algorithm to solve the equation system in $O(nJ^n)$ operations (for $J \sim 100$ and 1ns/op)

Degrees of Freedom n	1	3	6	9	12 (one H_2)	21 (one HeH^+)
Time to finish the computation	$10\mu\text{s}$	0.3s	1 week	28 528 years	2.78 times the age of the Universe	$> 10^{30}$ years (the last nucleon of the Universe long ago decayed)

2.5 The Actual Code Implementation

The source code of all the algorithms exposed in this work was implemented from scratch in a series of scripts in C++ managed by *Bash* scripts in *Linux*. Plots were generated using *gnuplot* scripts. All the algorithms were implemented in a same integrated environment controlled by a user interface, all of which was programmed *ad hoc*. It must be said that the author is currently working on a graphical user interface and an adaptation of the script flow for *Windows*, in order to offer it as free source for academic or research purposes. In principle, this dissertation shall not be centered in the inner workings of the implementations, but all the code is posted in the following open *Github* repository of the author: https://github.com/Oiangu9/The_Quantum_Many_Body_Problem_Bachelors_Thesis-.⁶

It must be noted that all the algorithmic implementations were also done in *Python* first, but attending the time consuming computations, in the end everything was rewritten down to C++, a low level compiled language, which made all the simulations several orders of magnitude faster (almost three orders). In particular, the algebraic part of the routines was implemented using the *Eigen* C++ library, which was crucial for a fast LU decomposition for instance.

2.6 Computing Bohmian Trajectories using the Wavefunction

Once one has an explicit expression for the dynamics of a wave-function (even if it is just numerical), it could be argued that obtaining Bohmian Trajectories has no use, as they will simply describe the density current lines, which can already be insights from a plot of the same dynamic density profiles. That is, once we obtain a profile by an algorithm such as the Cranck-Nicolson (CN) one, the computation of trajectories is somewhat *a posteriori*. Nonetheless, we have seen in the fist section of

⁶In a repository of this same account, once the *Windows* software is developed, a user guide and all the documentation and packages will be posted (presumably by the beginning of autumn).

the work that understanding the flow of these trajectories is very enlightening when it comes to build an intuition on quantum dynamics. We will use some examples of the CN implementation in order to illustrate this.

The first way one would try to compute the trajectories would be by using the (GL) straight away. That is, deriving numerically the phase of the obtained wave-function ($v_k = \frac{\partial S}{\partial q_k}$). This however, turns out to be numerically problematic, due to the fact that the phase of the wave-function is bounded in its main branch ($S \in [-\pi, \pi]$), which makes it have a discontinuity whenever the phase arrives to the edge of this domain. At first, I tried to correct this, by applying a post-treatment to the wave-vector's phase, by which the phase was made as continuous as possible (extending the phase to other branches). Although this was possible in 1D, it was concluded infeasible in 2D, where there are infinitely many directions in which we could force the phase to be continuous. In the end, it was decided that the best idea was to use the equivalent expression for the velocity fields given by the current densities J_k , defined as in classical fluid mechanics:

$$J_k(\vec{q}, t) := v_k(\vec{q}, t) \rho(\vec{q}, t) = v_k(\vec{q}, t) |\psi(\vec{q}, t)|^2$$

where using that $v_k(\vec{q}, t) = \frac{\partial S(\vec{q}, t)}{\partial q_k}$ it can be seen[1] that:

$$J_k(\vec{q}, t) = \frac{i\hbar}{2m_k} \left(\psi \frac{\partial \psi^\dagger}{\partial q_k} - \psi^\dagger \frac{\partial \psi}{\partial q_k} \right) = \frac{\hbar}{m_k} \operatorname{Im} \left(\psi^\dagger \frac{\partial \psi}{\partial q_k} \right)$$

which leads to an expression for the calculation of the velocity field for the k -th dimension:

$$v_k(\vec{q}, t) = \frac{\hbar}{m_k |\psi|^2} \operatorname{Im} \left(\psi^\dagger \frac{\partial \psi}{\partial q_k} \right) = \frac{\hbar}{m_k} \operatorname{Im} \left(\psi^{-1} \frac{\partial \psi}{\partial q_k} \right)$$

Computationally it is not as desirable as the (GL), as it implies a division by the density (which turns out to be very small in magnitude in most of the grid and could introduce numerical errors easily). Also, instead of numerically deriving a real function, we are now deriving a complex function. But the point is it does not give the discontinuity problem.

Note that all the derivatives in the work were carried out (for the central discrete points in the axis) using a fourth order central finite difference scheme given by:

$$\frac{df(x_i)}{dx} \simeq \frac{1}{12\Delta x} (-f(x_i + 2\Delta x) + 8f(x_i + \Delta x) - 8f(x_i - \Delta x) + f(x_i - 2\Delta x)) + O(\Delta x^4)$$

For the points in the grid boundaries, a typical second order central difference ($O(\Delta x^2)$) and a forward and backward $O(\Delta x)$ difference were used (for the outermost and second most outermost grid points in the axis).

Defining $\vec{v} := (v_k)_{k=1}^n$, the integration of the trajectories was performed using an Euler Method:

$$\vec{q}(t_i + \Delta t) \simeq \vec{q}(t_i) + \Delta t \vec{v}(\vec{q}(t_i), t_i)$$

2.7 Simulation Examples: How Trajectories approximate the Probability Density

If one begins with an ensemble of M trajectories chosen according to the probability distribution of the wave-function, then it can be shown [12] that in the limit of infinite trajectories, the ensemble approaches to the probability density of the quantum system at **any** subsequent time (which is natural given their interpretation):

$$|\psi(\vec{q}, t)|^2 = \lim_{M \rightarrow \infty} \frac{\sum_{n=1}^M \vec{q}(t) \delta(\vec{q} - \vec{q}(t))}{M}$$

This will be crucial for the third section's convergence proof.

It must be known that the most impressive and insightful results of the present work are the dynamical simulations realized. But it turns out that we cannot insert a dynamic animation in a paper, which might make a bit poor the resulting representations. In any case, all the animations performed for the realization of the images in the work are uploaded in the previously mentioned [repository](#). The reader is encouraged to check them while reading this.

All the simulations were achieved using atomic units (with $\hbar = 1$) and every mass set to $m_k = 1$. The exact grid and functional parameters used in the simulation of each figure are listed in [Appendix D](#).

n=1 : The Square Potential Barrier

Using the 1D CN algorithm derived above, we can make a fast study of the transmittance of a Gaussian wave-packet across a step potential. Setting the initial wave-packet and the potential in atomic units:

$$\psi(x, t = 0) = \frac{1}{\sqrt[4]{\pi\sigma^2}} e^{ik_0 x - \frac{(x-\mu)^2}{2\sigma^2}} \quad V(x, t) = \begin{cases} V_0 & \text{if } x \in [a, b] \\ 0.0 & \text{else} \end{cases}$$

With $V_0 = 10$, $a = 0$, $b = 2$ and $\sigma = 1.0$, $\mu = 3.0$, we vary the initial momentum k_0 and see the response. We choose randomly M initial points in x according to the probability density $|\psi(x, 0)|^2$. As we evolve the wave-function with the CN algorithm, we will evolve them as well. We can see for $M = 120$ and $k = 4.5$ some snapshots of the time evolution of ψ and the integrated trajectories in Figure 4. Note how, trajectories do not cross in configuration space, and they allow to imagine the motion of the wave-packet. Also, see how quantum tunneling across the barrier takes place in Fig.4, where some of the trajectories cross the barrier and others not. The typical exponential damping inside the wall can be seen as well.

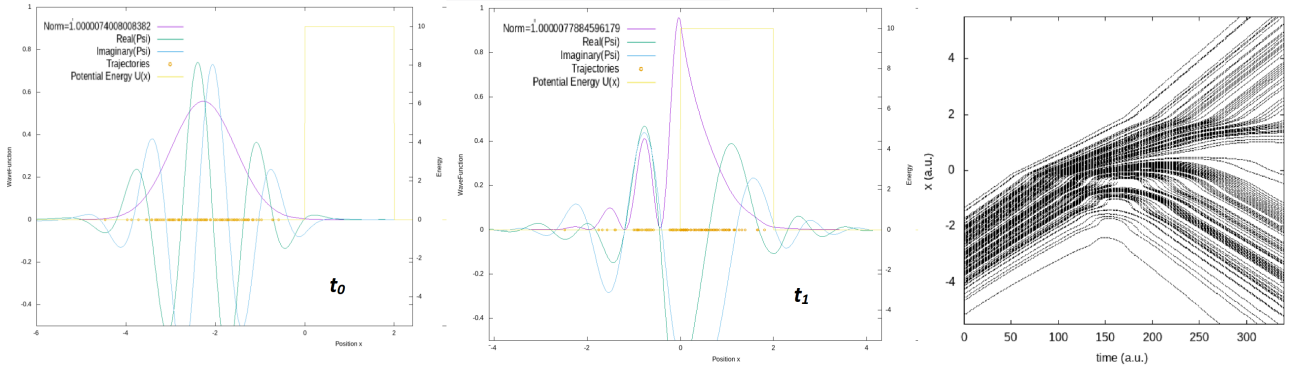


Figure 4: In the left, the initial state of the wave-packet before the collision, in the middle during the impact. The potential wall is in yellow, in purple the probability density, green, the real part of the wavefunction and blue the imaginary part. Trajectories at those times plotted as dotts in yellow. In the right the obtained Bohmian trajectories.

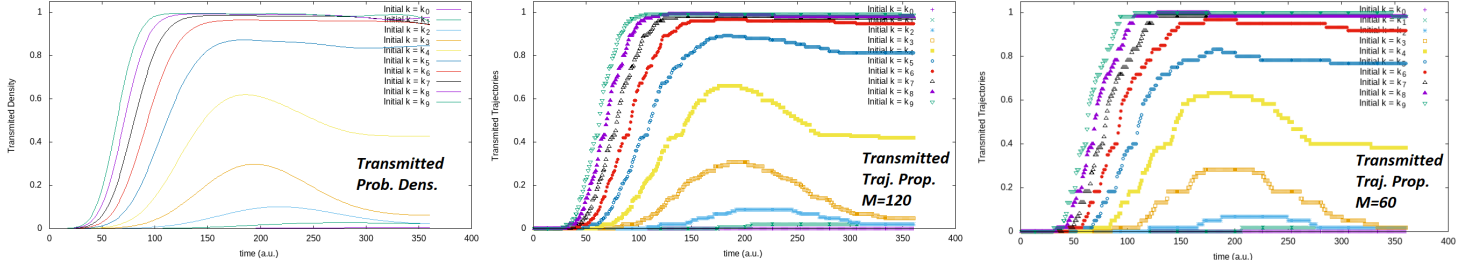


Figure 5: For different initial k_0 listed in Table 6, we see the transmitted probability density in the left and the transmitted trajectory percentage in the center (for $M = 120$) and right ($M = 60$). Note how, more trajectories make the transmitted proportion curves more similar to that of density.

We check in particular the transmitted probability density percentage and the transmitted Bohmian trajectory percentage at each time for several initial momenta k_0 , for $M = 60$ and $M = 120$ (Figure 5). It can clearly be seen that the absolute difference of the transmission measurement using trajectories and using the probability density get closer to each other with increasing number of trajectories, following the mentioned intuition. Also, the bigger the initial k_0 the higher the final transmitted proportion, approaching an asymptotic limit, as it can be expected from theoretical grounds, see Ref.[13].

n=2 : The Double Slit Interference

Using the 2D CN algorithm we can simulate a single electron crossing a double slit and see the interference pattern its probability-density generates. The double slit could be modeled using an infinite wall with two apertures, but abrupt potential breaks cause numerical instabilities. Instead, using a Gaussian wave in x and two inverted Gaussians in the y , a smoother step can be obtained.

Considering:

$$\psi(x, y, t = 0) = \frac{1}{\sqrt[4]{2\pi\sigma_x\sigma_y}} e^{ik_xx - \frac{(x-\mu_x)^2}{4\sigma_x^2}} e^{ik_yy - \frac{(y-\mu_y)^2}{4\sigma_y^2}} \quad (2DG)$$

$$V(x, y) = \frac{V_0}{\sqrt{2\pi}\sigma_0} e^{\frac{x^2}{2\sigma_0^2}} \left(E_0 - \frac{1}{\sqrt{2\pi}} \left(\frac{1}{\sigma_1} e^{\frac{(y-\mu_1)^2}{\sigma_1^2}} + \frac{1}{\sigma_2} e^{\frac{(y-\mu_2)^2}{\sigma_2^2}} \right) \right)$$

Using $\sigma_0 = 0.5$, $\sigma_1 = 0.6$, $\sigma_2 = \sigma_1$, $\mu_1 = 1.5$, $\mu_2 = -\mu_1$, $V_0 = 40.0$ and $E_0 = \frac{1}{\sigma_1\sqrt{2\pi}}$ and centering the wave-packet at $(-6, 0)$ with an initial momentum $k_x = 6.0$ and $k_y = 0$, we get a pleasant animation of which we put some shots in Figure 6. We used $M = 150$ trajectories (chosen according to ρ_0).

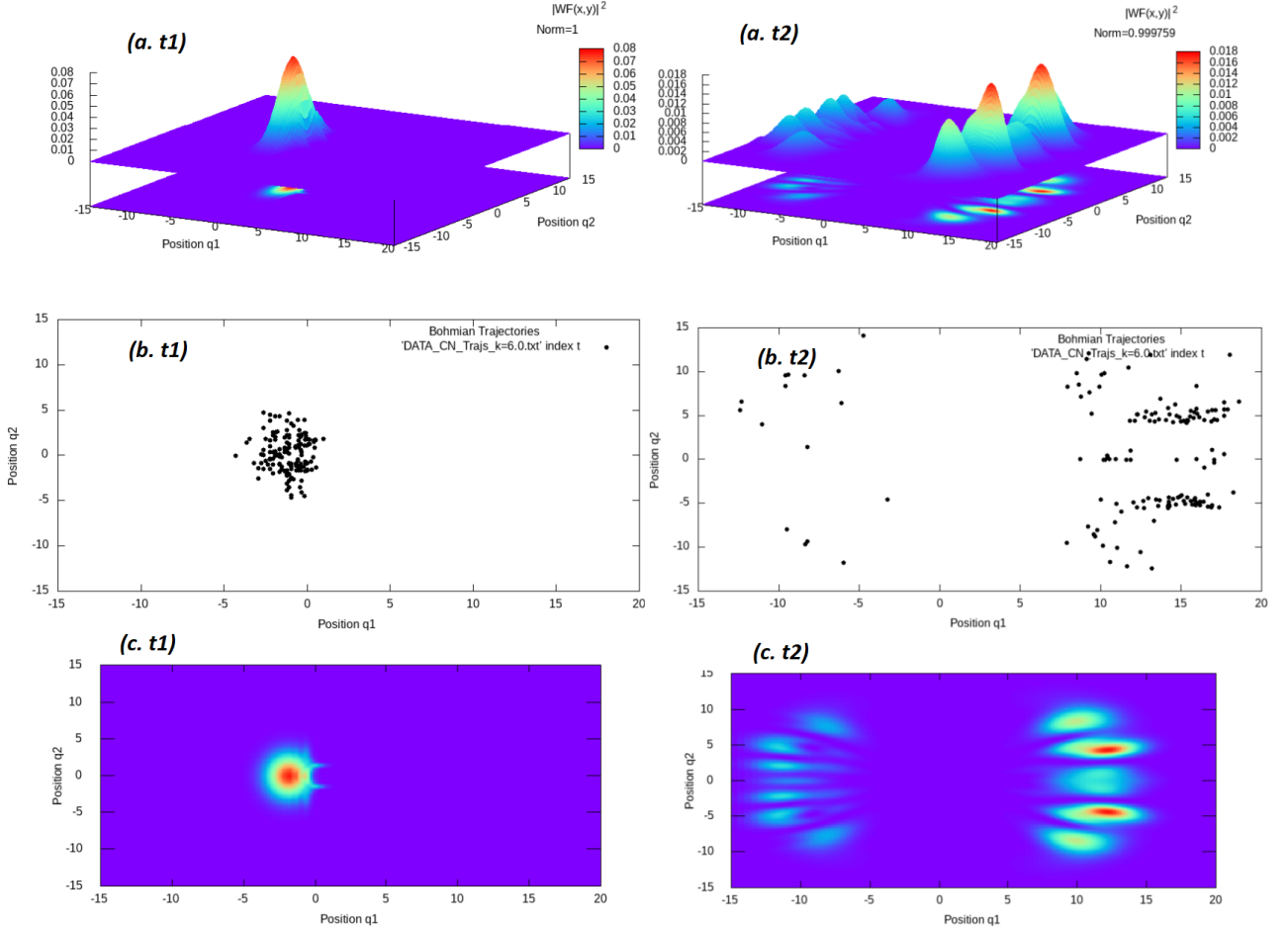


Figure 6: For two instances $t1 < t2$: probability density plots (3D in (a) and color map in (c)) together with the trajectories (the (b)). Evolution using 2D CN. See the emergence of the interference pattern (which obviously is represented in the trajectories as well). The norm at both times in the inset of (a), check that the evolution was unitary.

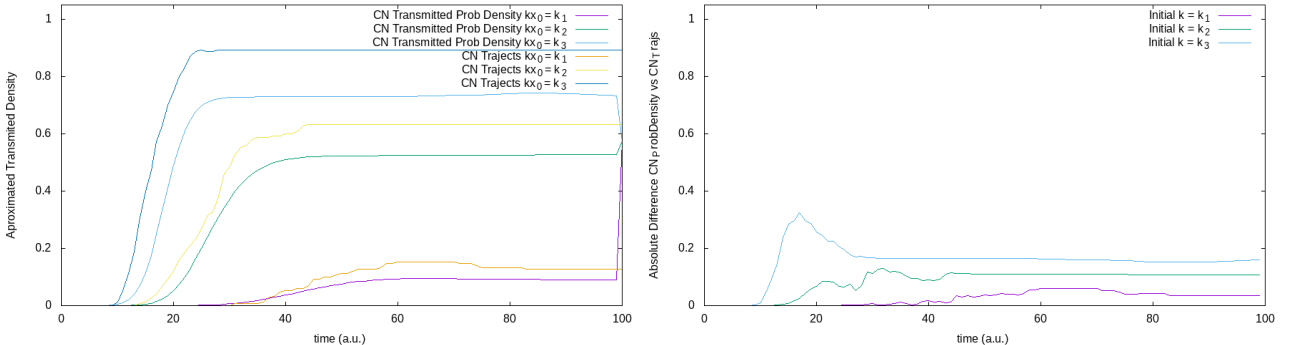


Figure 7: For different initial k_0 listed in Table 6, we see the transmitted probability density vs the transmitted trajectory percentage in the left and the absolute difference between them in the right for $M = 150$.

We analyze the percentage of probability density transmitted through the slits and the percentage of trajectories that crossed them, for each time and three different initial momenta in Figure 7. Once again, see how close the measurements happen to be if using the approximation of the trajectories instead of the “exact” probability density.

3 The Conditional Single Particle Wavefunction Decomposition: An exponential problem turned into polynomial?

We have clearly seen both on theoretical and numerical grounds, that there is a problem in the time evolution of a quantum system with increasing number of dimensions (degrees of freedom). We proved that trying to solve the **SE** “exactly”, becomes absurd both spatially and temporally for systems with more than a very small number of dimensions. Therefore, approximations are a practical necessity.

Using the exclusive viewpoint Bohmian Mechanics gives us in order to understand quantum particle trajectories, it is possible to find a very interesting and quite unknown decomposition of the n -dimensional **SE** into a system of n coupled 1D Schrödinger like equations. This very unexplored framework will allow us to develop original algorithms to face the N body problem.

3.1 The Conditional Single Particle Wavefunction Decomposition

Given $\vec{q} = (q_1, \dots, q_n) \in \mathbb{R}^n$ are the n spatial dimensions or degrees of freedom of our quantum system, let us consider a particular trajectory for every dimension except the a -th as:

$$\vec{q}_b(t) := (q_1(t), \dots, q_{a-1}(t), q_{a+1}(t), \dots, q_n(t))$$

Recalling the n dimensional wave-function $\Psi(\vec{q}, t) = R(\vec{q}, t)e^{S(\vec{q}, t)/\hbar}$, solution of the **SE**, $\vec{q}_b(t)$ is a trajectory following the velocity field defined by this wave-function and the **(GL)**. We define by a **Single Particle Conditional Wave Function (SPCWF)** the full n dimensional wavefunction conditioned to that particular trajectory, for every variable except the a -th. That is:

$$\Phi_a(q_a, t) := \Psi(q_a, t; \vec{q}_b = \vec{q}_b(t))$$

Then, we could write this SPCWF in polar form by defining its amplitude and phase as the conditionals of the full wave-function:

$$\Phi_a(q_a, t) = \Psi(q_a, t; \vec{q}_b(t)) = R(q_a, t; \vec{q}_b(t)) e^{S(q_a, t; \vec{q}_b(t))/\hbar} = r_a(q_a, t) e^{\mathcal{S}_a(q_a, t)/\hbar} \quad (\text{SPCWF})$$

$$r_a(q_a, t) = R(q_a, t; \vec{q}_b(t))$$

$$\mathcal{S}_a(q_a, t) = S(q_a, t; \vec{q}_b(t))$$

One can interpret $|r|^2$ as a typical conditional probability density. \mathcal{S} would be the action value \mathbb{S} , fixing the upper end points for all the coordinates to $\vec{q}_b(t)$ at each time (leaving only q_a free).

This SPCWF may have nothing to do with the full wave-function except that its partial derivative with respect to q_a will coincide with the full wavefunction’s (if this last was conditioned to $\vec{q}_b(t)$). Then, the SPCWF can be used to obtain the exact same Bohmian velocity field for q_a that would have been obtained from the full wavefunction (if the rest of the coordinates gave a trajectory $q_b(t)$). In essence, using $\mathcal{S}_a(q_a, t)$, as if it really was a single 1D particle we can evolve the trajectory for q_a :

$$\frac{dq_a(t)}{dt} = \frac{1}{m_a} \frac{\partial S(q_a, t; \vec{q}_b)}{\partial q_a} \Big|_{\vec{q}(t)=(q_a(t), \vec{q}_b(t))} = \frac{1}{m_a} \frac{\partial S(q_a, t; \vec{q}_b(t))}{\partial q_a} \Big|_{q_a(t)} = \frac{1}{m_a} \frac{\partial \mathcal{S}_a(q_a, t)}{\partial q_a} \Big|_{q_a(t)}$$

Therefore, the single dimension q_a is guided by a truly spatially 1D velocity field:

$$v_a(q_a, t) = \frac{1}{m_a} \frac{\partial \mathcal{S}_a(q_a, t)}{\partial q_a}$$

Thus we have that the 1D wavefunction Φ_a guides the trajectory of the coordinate q_a as if it was an actual single particle. But what about the time evolution of the apparently single particle wavefunction itself $\Phi_a(q_a, t)$? Well, it can be proved that it also follows an equation that is almost like the Schrödinger Equation for a 1D particle. Of course, if the system is not factorisable, the resulting equation cannot be a proper 1D SE, as if not the quantum entanglement between the dimensions would be lost. Nevertheless, at the expense of two additional (very complicated) terms in the 1D SE's potential, this can indeed be done. That is, it is possible to dismantle the n dimensional SE into n **coupled single particle Pseudo Schrödinger Equations**(PSE). For each $a \in \{1..n\}$ and $\vec{q}_b = \vec{q} \setminus q_a$:

$$i\hbar \frac{\partial \Phi_a(q_a, t)}{\partial t} = \left[\frac{\hbar^2}{2m_a} \frac{\partial^2}{\partial q_a^2} + \mathcal{U}_a(q_a, t; \vec{q}_b(t)) + G_a(q_a, t; \vec{q}_b(t)) + i J_a(q_a, t; \vec{q}_b(t)) \right] \Phi_a(q_a, t) \quad (\text{PSE})$$

$$\frac{dq_a(t)}{dt} = v_a(q_a, t) = \frac{1}{m_a} \frac{\partial \mathcal{S}_a(q_a, t)}{\partial q_a}$$

where the derivation of these equations following [1], the definition of the potential energy terms G_a , J_a and \mathcal{U}_a with their deepest implications are exposed in **Appendix E**. The most interesting part about this development is that, using conditional wave-functions, one can describe a sub-system separately of the full quantum system, which Orthodox QM fails to allow. This is one of the strongest points of Bohmian Mechanics: all the entanglement and correlations of a sub-system with the rest of the system are gathered in those potential energy terms. The particle is evolved as a single particle otherwise! All the complex environment is treated as a potential energy influence (no need of any reduced density matrix)! Against the Orthodox criticism, trajectories have now become non-superfluous. But note that this does not mean one can evolve trajectories without the wave-function. The expressions for G_a and J_a still need information of the full wave-function, so the many body problem is still there, just that it is now concealed, and has maybe a more intuitive look. The point is that the conditioning of the wave-function is an irreversible operation, which means we cannot rebuild the full wave-function even if we knew the SPCWF $\Phi_a \forall a$ (if we know them for several trajectories then the story is different).

However, approximating the SE has now been traduced into approximating G_a and J_a . We now are even allowed to make approximations in the single dimension scale: *ad hoc* as a function of the nature of each dimension q_a ! No matter if one accepts Bohmian mechanics or not, this development is exact. Thus, similar to the work on DFT, *the theory is exact, but the solutions will be approximate*.

3.2 Algorithm A: The Zero-th Order Taylor Expansion of G_a and J_a

In this section the simplest possible approximation to the (PSE) for a system of N particles with correlation (inter-dependences in the potential energy -factorizability banned-) but without exchange interaction (that is, where the coordinates/particles are distinguishable -no identical particles-) will be provided. That is, a system where the correlation source is mainly “geometrical” -due to the potential \mathcal{U}_a . This algorithm was developed by X. Oriols [14], and we will simply re-justify it and retest it here following his development.

In principle, as we are only interested in using the SPCWF to compute one trajectory, $q_a(t)$, it appears natural to consider the vicinity of the trajectory $q_a(t)$ for the G_a and J_a terms. Developing a Taylor expansion of them in q_a , around the point $q_a(t)$ in each time:

$$\begin{cases} G_a(q_a, t) = G_a(q_a = q_a(t), t) + \frac{\partial G_a(q_a, t)}{\partial q_a} \Big|_{q_a(t)} (q_a - q_a(t)) + \dots \\ J_a(q_a, t) = J_a(q_a = q_a(t), t) + \frac{\partial J_a(q_a, t)}{\partial q_a} \Big|_{q_a(t)} (q_a - q_a(t)) + \dots \end{cases} \quad \text{for } q_a \rightarrow q_a(t)$$

Here, the higher the number of terms used, the better the approximation would be. Each time more and more of the exchange and entanglement would be captured. Nonetheless, the simplest case will be to consider just the zero order terms:

$$\begin{cases} G_a(q_a, t) \approx G_a(t; q_a(t)) \\ J_a(q_a, t) \approx J_a(t; q_a(t)) \end{cases}$$

This yields an approximated equation system: for $a \in \{1..n\}$ and $\vec{q}_b = \vec{q} \setminus q_a$

$$i\hbar \frac{\partial \Phi_a(q_a, t)}{\partial t} = \left[\frac{\hbar^2}{2m_a} \frac{\partial^2}{\partial q_a^2} + \mathcal{U}_a(q_a, t; \vec{q}_b(t)) + G_a(t; \vec{q}(t)) + i J_a(t; \vec{q}(t)) \right] \Phi_a(q_a, t)$$

The fun point of this approximation is that now G_a and J_a are **purely time dependent potential terms**, as happens in the exact factorizable wavefunction case (see Sect. V.6.2 in [1])! As such, acknowledging that a real or imaginary purely time dependent potential term added into the Hamiltonian of the **SE** only introduces a purely time dependent global phase in the wave-function Φ_a : their presence or absence yields a SPCWF Φ_a that generates the same velocity field for q_a . As the velocity field has to do with a spatial derivative of the phase, the purely time dependent term is a constant for the partial derivative. Therefore, if we simply avoid calculating explicitly G_a and J_a , we will actually be accounting for them up to first order.

Then, a simple algorithm can be proposed (setting $G = 0$ and $J = 0$) that even if it looks like it is treating the system as separable it is actually taking into account some geometric correlations, thanks to the term \mathcal{U}_a , which depends on the rest of particles $\vec{q}_b(t)$:

$$i\hbar \frac{\partial \phi_a(q_a, t)}{\partial t} = \left[\frac{\hbar^2}{2m_a} \frac{\partial^2}{\partial q_a^2} + \mathcal{U}_a(q_a, t; \vec{q}_b(t)) \right] \phi_a(q_a, t) \quad (\text{Alg.A})$$

with $a \in \{1..n\}$ and $\vec{q}_b = \vec{q} \setminus q_a$

They are n equations coupled in a simple way through their trajectories. This is the master equation for Algorithm A (Alg.A). Its resolution would just follow: given an initial state of the full wave-function $\Psi(\vec{q}, t_0)$ and an initial point of the system trajectory $\vec{q}(t_0)$, first compute the SPCWF-s for each a as $\phi_a(q_a; t_0) = \Psi(q_a; t = t_0, \vec{q}_b(t))$. Then compute a time iteration for each of the equations (by using for instance a 1D CN), and use the phases of the SPCWF-s in this time to compute the velocity fields that will evolve the trajectory to this new time step. Now, redefine the propagator operators using the new trajectory position (as the potential energies \mathcal{U}_a depend on $\vec{q}_b(t)$), and compute another time iteration for each of the SPCWF-s. Reiterate for each considered time step. This was implemented in my case by evolving n 1D Cranck Nicolson equations in parallel, updating in each iteration the U_L and U_R matrices using the new shape of \mathcal{U}_a per each dimension a .

Despite its simplicity, the present approximation is already a breakthrough, because it allows to obtain *non a posteriori* trajectories like it is possible in classical mechanics. Here we need no full wave-function for quantum dynamics!

We must insist that the SPCWF-s of a single trajectory need not reproduce the true n -particle Ψ : the only “meaningful” information obtained, a priori, will be the global trajectory $\vec{q}(t)$. However, as previously commented, if one needed information about the whole n wave-function, one could simply compute different trajectories, initiating them according to the probability distribution of the initially known Ψ . From the trajectory ensemble it is easy to know the dynamical behaviour of the full wavefunciton. Moreover, we could use the SPCWFs of different trajetcories to rebuild the full wavefunction: by making a linear combination of the tensor products of SPCWFs evolved using different trajectories for instance. Work on this is still to be done, but a similar approach has been developed by G. Albareda et al.[15]. The current or energetic information can be easily obtained as well, as each trajectory is equivalent to a probability density current line.

In any case, we do not always need the full wave-function. The wave-function of the center of mass of a quantum system with many particles, appears to tend towards a Dirac delta when the number of particles is very big [16]. This means that under such conditions most of the Bohmian Trajectories of the center of mass will tend towards the expectation of the trajectories of the SPCWF of the center of mass. In such a limit, a single trajectory becomes more and more relevant. Thus, for the study of an electron flow in a transistor for instance⁷, it could arrive to be enough the use of an algorithm like **Alg.A**, centered in obtaining a single trajectory.

⁷Electrons are fermions, and would thus require a special treatment for their exchange interaction. Actually an adaptation of **Alg.A** to such a case can be found in [14]. But still the argument holds.

Computationally speaking, the algorithm requires a mathematically harder description, but way more efficient. Note that here, **the computational complexity only grows polynomially with dimensions!** The growth is no longer exponential! Adding new dimension only adds the resolution of an additional single particle SE! If using the Crank Nicolson algorithm for instance to calculate them, it would only imply an additional 1D U_L , U_R decomposition. Following the optimistic lower bound we gave in Section 2 instead of $O(nJ^{n+1})$, it would now be $O(n^2J^2)$, that is, n coupled 1D CN evolutions. It even allows multiple multiprocessing strategies. The computation of each iteration of each of the dimensions, or the computation of different trajectories could be done in parallel.

3.2.1 Testing the Algorithm: The Double Slit Experiment

Going back to the double slit experiment, it is a non-factorisable problem, so the Algorithm A is expected to yield only an approximation of the solution. Let us test it against the results we obtained using the 2D CN, which did not apply any approximation on the SE.

The two dimensions of this problem represent the degrees of freedom of one same particle, which means the quantum entanglement due to exchange interactions a priori will not be a problem. But still, it could be expected that the algorithm does not capture enough correlation as to yield the interference pattern (it treats the problem almost as if it was factorisable). We simulate exactly the same conditions as the ones in Section 2.7 (using CN) and we meet a surprise: the algorithm captures the interference pattern! The coupled evolution of the x and y SPCWF-s, seems to imprint enough correlation as to yield an interference. We evolved $M = 150$ trajectories using $k_x = 6.0$ in the initial wave-function. Some snapshots can be seen in Figure 8 (for full animations see the [repository](#)).

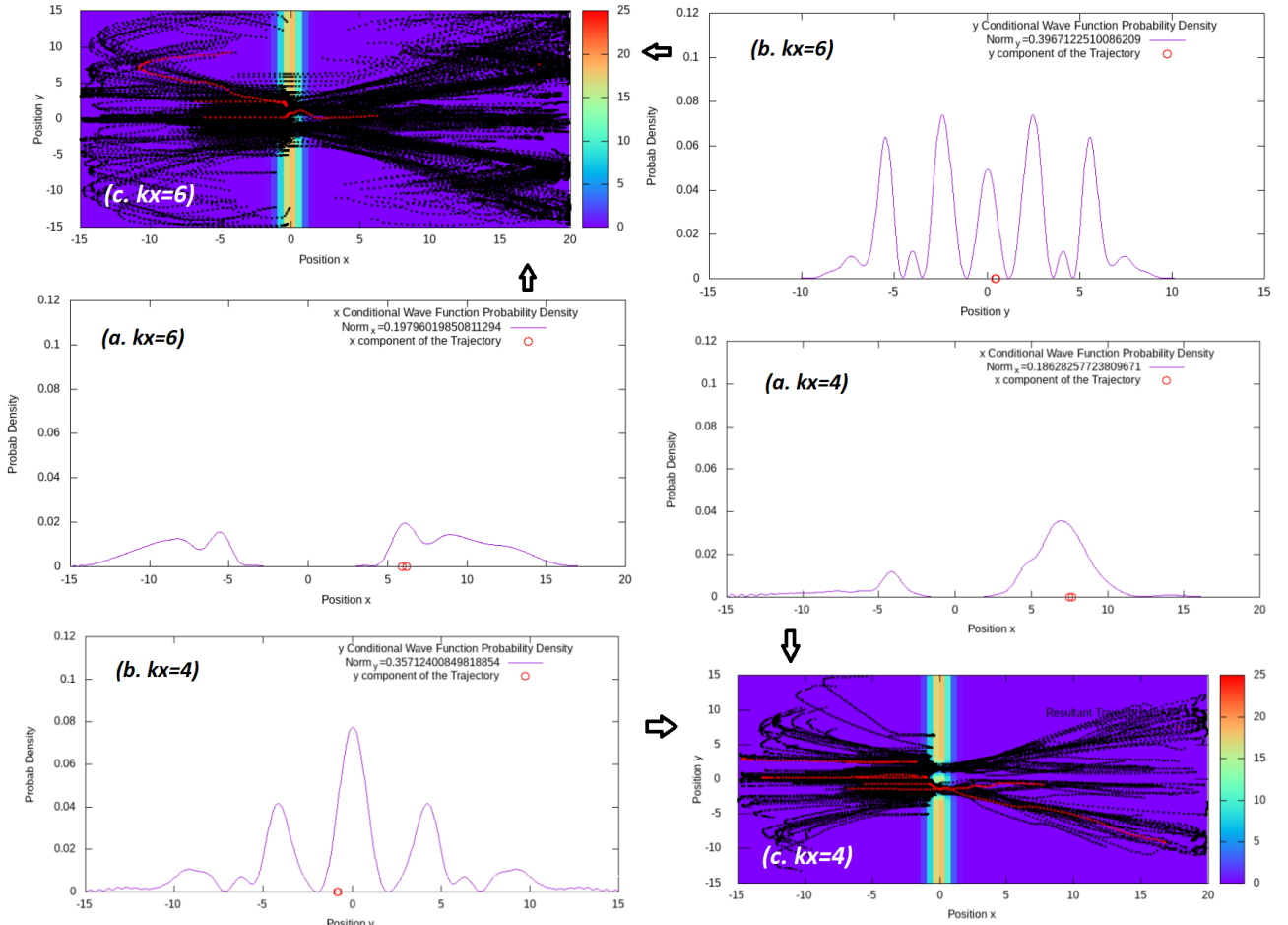


Figure 8: For $k_x = 4$ (with $M = 150$) and $k_x = 6$ (with $M = 350$): In (c) calculated trajectories (black lines) over a color map of the potential energy. Note how trajectories are reflected in the grid boundaries. The interference pattern can be seen in the shape of the trajectory ensemble and in (b): the probability density of the y -SPCWF $\Phi_y(y, t)$ for the trajectory in red that crossed the slits. (c) shows the same for the x -SPCWF $\Phi_x(x, t)$. Note how the norm of the SPCWF-s need not be conserved nor be unitary.

In order to ensure the quality of the trajectory prediction, we can perform a transmission comparison with the CN method. For this we will use on the one hand the probability density transmission of CN, and on the other hand, a fairer comparison using the trajectories computed with the CN result. One could argue that a more accurate test would be to directly compare the obtained particular trajectories instead of the transmission of the ensemble. However, there is an abyss of difference in the spatial grids used by both algorithms. While the 2D CN appears to have more than enough for norm convergence and stability with 300 divisions in each dimension (more would make calculations take too long), each SPCWF can easily have more than 500 divisions in each dimension. This means, that the discrete steps taken by the trajectories should not be expected to coincide. Instead, an alternative measurement like the current transmission seems more logical.

We can see in Figure 9 the comparison of the approximated transmissions of the wave-function using CN and the present algorithm. Amazingly the transmission percentages match way better for the SPCWF trajectories with the CN probability density (Fig.9), than the same probability density with the CN trajectories (Fig.7). This is probably due to the finner integration of trajectories in the SPCWF algorithm. In any case this clearly proves the quality of the approximation!

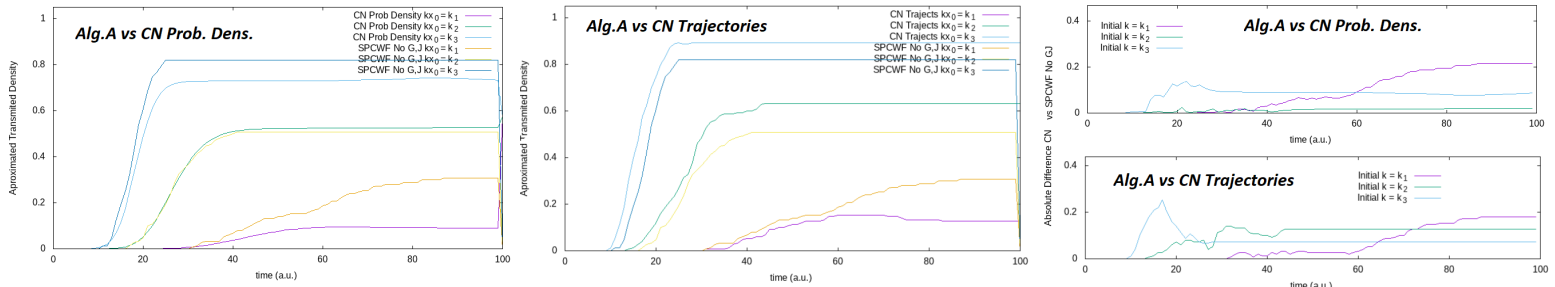


Figure 9: For different initial k_0 listed in Table 6, in the left the transmitted probability density using CN simulation vs the transmitted trajectory proportion with Alg.A for each time. In the middle the transmitted proportion with trajectories using CN vs Alg.A's. In the right the evolution of absolute differences per each of the k_0 in each case (using $M = 150$).

Actually, inspecting in Figure 8 the number of interference probability bulbs predicted by the **Alg.A** simulation using $k_0 = 6.0$, and inspecting this in the “exacter” CN in Figure 6, we see that both present 5 bulbs! An excellent match for an algorithm that was not supposed to capture correlations. In the animations in the [repository](#) of the work, you can find this same correspondence also for the case of $k_0 = 4.0$, where one can see between 3 and 4 bulbs in both cases.

In front of the present success of the algorithm to capture the physics of a **non** factorisable system so neatly, even if not accurately, it was a natural consequence to center the attention of the subsequent developments on the geometrical points that allowed it. In particular, there is a geometrical correlation that **Alg.A** is not able to capture in the moment the slits are crossed. Due to the resonant modes of the tunnel, even if the slit is open and $\mathcal{U}_a = 0$, there is a virtual barrier that impedes the entrance for packets with lower energy than this barrier energy. Using only \mathcal{U}_a this important correlation in electronics cannot be captured. The following approach was developed, with the motivation to overcome this finding.

3.3 Algorithm B: The Born-Huang Expansion and Adiabatic States

The algorithm we will be presenting here is a completely nouvelle approach in the scientific literature developed in the last months by X. Oriols and G. Albareda, which I have been the honor to be the one implementing and testing (and dealing with the gore details) for the very first time. As these are the initial steps in the development, even if the algorithm will be extensible to arbitrary dimensions, we will center ourselves in a 2 dimensional case.

3.3.1 The Born-Huang expansion and the Adiabatic States

Given a system with two 1D particles or a single 2D particle, the time dependent SE governing the motion of its wave-function $\psi(x, y, t)$ in a time independent potential V reads:

$$i\hbar \frac{\partial \psi}{\partial t} = H(x, y, t)\Psi \quad (2DSE)$$

s.t. $H(x, y, t) = -\frac{\hbar^2}{2m_x} \frac{\partial^2}{\partial x^2} - \frac{\hbar^2}{2m_y} \frac{\partial^2}{\partial y^2} + V(x, y)$. We could consider a time dependent potential as well, but since we will perform the whole analysis on a stationary potential, to begin with it is more convenient to leave it this way.

Then, let us define the set $\{\varphi_x^j(y)\}_{j=0}^\infty$, as the eigenstates of the Hamiltonian of a particular section in the x axis (thus the parameter x in the eigenstates). Given the section Hamiltonian $H_x(y)$:

$$H_x(y) = -\frac{\hbar^2}{2m_y} \frac{\partial^2}{\partial y^2} + V(y; x)$$

its eigenstates satisfy:

$$H_x(y)\varphi_x^j(y) = E_x^j\varphi_x^j(y)$$

where E_x^j is the j -th smallest eigenvalue of $H_x(y)$ (also parametrized by x).

In short, we have that $\varphi_x^j(x)$ are the eigenstates of the system if it was restricted to a certain x value. We now consider the so called **Born-Huang expansion**(BHE) of the full wave-function:

$$\psi(x, y, t) = \sum_{j=0}^{\infty} \chi^j(x, t)\varphi_x^j(y) \quad (BHE)$$

That is, we define the value of ψ at each x position as a linear combination of functions that form a complete orthogonal basis of the spatial dimension y : the $\varphi_x^j(y)$ (as they are the eigenstates of a hermitian operator $H_x(y)$). We call the states $\{\varphi_x^j(y)\}_{j=0}^\infty$ and the coefficients $\chi^j(x, t)$, the **adiabatic states** and **adiabatic coefficients** respectively⁸. Let us define the quantity $\Lambda := \sum_{j=0}^{\infty} \int_{-\infty}^{\infty} |\chi^j(x, t)|^2 dx$. As proved in **Appendix C**, it should fulfill $\Lambda = 1$ due to the normalization of ψ .

3.3.2 Adiabatic states for the simple infinite wall geometric constriction

Let us imagine a system of one particle in two dimensions, which are linked to each other through a potential $V(x, y)$ that allows an almost free transport of the particle in the x direction, but makes it be bounded in the y direction. In particular we consider a system in which the particle in y is confined by an infinite potential of length $L(x)$ that will depend on its position in the x axis. This is the description of a conducting 2D channel for an electron with possible irregularities in the width of the channel (the y direction), or a single slit diffraction experiment (the impinging particle on the slit is confined in the y direction when crossing the slit).

The point is that in such a potential, the eigenstates of sections in the x axis are trivial sinusoids: each of the section Hamiltonians would describe a 1D particle in an infinite potential box (of width $L(x)$). Thus, we would have that the analytical expression for the adiabatic states would be:

$$\varphi_x^j(y) = \sqrt{\frac{2}{L(x)}} \sin\left(\frac{j\pi}{L(x)}y\right) \text{ with } j = 0, 1, 2, \dots \quad (PIB)$$

with eigenvalues $E_x^j = \frac{j^2\pi^2\hbar^2}{2m_x L(x)^2}$. Note that in this particular case $\forall j$, the $\varphi_x^j(y)$ are real functions!

3.3.3 The Master Equation of the Algorithm: the Born-Huang expansion into the SE

If we take a trajectory $(x_a(t), y_a(t))$ following the (GL) for the $n = 2$ case, we can condition the whole 2D wave-function to $y_a(t)$ and obtain the x -SPCW $\phi_{y_a}(x, t)$, or to $x_a(t)$ for the y -SPWF $\phi_{x_a}(y, t)$. Evaluating the Born-Huang expansion in the x -SPCW $\phi_{y_a}(x, t)$:

$$\phi_{y_a}(x, t) := \psi(x, t; y = y_a(t)) = \sum_{j=0}^{\infty} \varphi_x^j(y_a(t))\chi^j(x, t) \quad ; \quad \phi_{x_a}(y, t) := \psi(y, t; x = x_a(t))$$

⁸At this point, note that if the potential V was time dependent, then so would be the section Hamiltonian $H_x(y)$. As a consequence, the adiabatic states $\{\varphi_x^j\}_j$ and the section energies $\{E_x^j\}_j$ would have a different shape at each time, and thus another parameter should be added to them. But the discussion would still hold.

Such that:

$$\frac{dy_a(t)}{dt} = \frac{1}{m_y} \frac{\partial S(y, t; x_a(t))}{\partial y} \Big|_{y_a(t)} \quad \frac{dx_a(t)}{dt} = \frac{1}{m_x} \frac{\partial S(x, t; y_a(t))}{\partial x} \Big|_{x_a(t)}$$

Recalling the derivation of (PSE), we take the (2DSE) and evaluate it along a trajectory $y_a(t)$:

$$i\hbar \frac{\partial \psi(x, y, t)}{\partial t} \Big|_{y_a(t)} = \left[-\frac{\hbar^2}{2} \left(\frac{1}{m_x} \frac{\partial^2}{\partial x^2} + \frac{1}{m_y} \frac{\partial^2}{\partial y^2} \right) + V(x, y) \Big|_{y_a(t)} \right] \psi(x, y, t) \Big|_{y_a(t)}$$

Noting that: $\frac{\partial \psi(x, t; y_a(t))}{\partial t} = \frac{\partial \psi(x, y, t)}{\partial t} \Big|_{y_a(t)} + \frac{\partial \psi(x, y, t)}{\partial y} \Big|_{y_a(t)} \frac{dy_a(t)}{dt}$ and $\frac{\partial \psi(x, t; y_a(t))}{\partial t} = \frac{\partial \phi_{y_a}(x, t)}{\partial t}$:

$$i\hbar \frac{\partial \phi_{y_a}(x, t)}{\partial t} = \left[-\frac{\hbar^2}{2m_x} \frac{\partial^2}{\partial x^2} + V(x; y_a(t)) \right] \phi_{y_a}(x, t) - \frac{\hbar^2}{2m_y} \frac{\partial^2 \psi(x, y, t)}{\partial y^2} \Big|_{y_a(t)} + i\hbar \frac{\partial \psi(x, y, t)}{\partial y} \Big|_{y_a(t)} \frac{dy_a(t)}{dt}$$

Which is a non-linear and non-unitary DE. But notice that going back to PSE we could identify:

$$G(x, t; y_a(t)) \phi_{y_a}(x, t) = -\frac{\hbar^2}{2m_y} \frac{\partial^2 \psi(x, y, t)}{\partial y^2} \Big|_{y_a(t)} \quad \text{and} \quad J(x, t; y_a(t)) \phi_{y_a}(x, t) = \hbar \frac{\partial \psi(x, y, t)}{\partial y} \Big|_{y_a(t)} \frac{dy_a(t)}{dt}$$

Let us call them the **Kinetic** and **Advection Correlation Potentials** respectively. Notice that **here is the geometrical correlation we were looking for!** Pay attention to the real potential G . In the case of the slit, the adiabatic states $\varphi_x^j(y)$ are the sinusoids (PIB) of the infinite box, thus as $\psi(x, y, t)$ was expanded as a sum of these states (BHE), for the case of the slit/tunnel:

$$G(x, t; y_a(t)) \phi_{y_a}(x, t) = -\frac{\hbar^2}{2m_y} \frac{\partial^2}{\partial y^2} \left(\sum_{j=0}^{\infty} \chi^j(x, t) \varphi_x^j(y) \right) \Big|_{y_a(t)} = -\frac{\hbar^2}{2m_y} \sum_{j=0}^{\infty} \chi^j(x, t) \left(-\sqrt{\frac{2}{L}} \frac{j^2 \pi^2}{L^2} \sin\left(\frac{j\pi}{L} y\right) \right) \Big|_{y_a(t)} = \sum_{j=0}^{\infty} \frac{\hbar^2 j^2 \pi^2}{2m_y L^2} \chi^j(x, t) \varphi_x^j(y_a(t))$$

where we can recognize the “particle in a box”-like energy terms $\frac{\hbar^2 j^2 \pi^2}{2m_y L^2}$ that are the ones causing the “virtual” barrier in the entrance we mentioned. The confinement in y has created a barrier in x !

Returning to the development of the master equation, until here all the development was exact. Let us now introduce the **only** approximation of the algorithm: we will assume for the computation of the χ^j coefficients that:

$$\psi(x, y, t) \approx \frac{\phi_{y_a}(x, t)}{\sqrt{N_x}} \frac{\phi_{x_a}(y, t)}{\sqrt{N_y}}$$

$$N_x := \int_{-\infty}^{\infty} |\phi_{y_a}(x, t)|^2 dx \quad N_y := \int_{-\infty}^{\infty} |\phi_{x_a}(y, t)|^2 dy$$

such that the normalization condition of the full wave-function is satisfied by construction. It is true that the wave-function is not factorisable in general, but this will **not** be an approximation on the time evolution of the SPCWF-s, but on the extraction of the χ^j terms. These coefficients will be used to estimate the correlation potentials G and J . That is, the approximation is on G and J .

Using Proposition 1 of Appendix C:

$$\chi^j(x, t) = \int \varphi_x^j(y)^\dagger \psi(x, y, t) dy \simeq \frac{1}{\sqrt{N_y N_x}} \int \varphi_x^j(y)^\dagger \phi_{y_a}(x, t) \phi_{x_a}(y, t) dy$$

where $\phi_{x_a}(y, t)$ is y independent, and thus defining the integrals:

$$U^j(x, t) := \frac{1}{\sqrt{N_y N_x}} \int \varphi_x^j(y)^\dagger \phi_{x_a}(y, t) dy$$

we are left with an approximation for the $\chi^j(x, t)$ and the full wave-function:

$$\chi^j(x, t) \simeq U^j(x, t) \phi_{y_a}(x, t)$$

$$\psi(x, y, t) \simeq \sum_{j=0}^{\infty} U^j(x, t) \varphi_x^j(y) \phi_{y_a}(x, t)$$

Where again, the only approximation is on the evaluation of the χ^j . This will allow us to obtain an expression for the Kinetic and Advective Correlation Potentials:

$$G(x, t; y_a(t)) \phi_{y_a}(x, t) = -\frac{\hbar^2}{2m_y} \frac{\partial^2 \psi(x, y, t)}{\partial y^2} \Big|_{y_a(t)} \simeq \left[-\frac{\hbar^2}{2m_y} \sum_{j=0}^{\infty} U^j(x, t) \frac{\partial^2 \varphi_x^j(y)}{\partial y^2} \Big|_{y_a(t)} \right] \phi_{y_a}(x, t)$$

$$J(x, t; y_a(t)) \phi_{y_a}(x, t) = \hbar \frac{\partial \psi(x, y, t)}{\partial y} \Big|_{y_a(t)} \frac{dy_a(t)}{dt} \simeq \hbar \frac{dy_a(t)}{dt} \left[\sum_{j=0}^{\infty} U^j(x, t) \frac{\partial}{\partial y} \varphi_x^j(y) \right] \phi_{y_a}(x, t)$$

And hence we have now explicit expressions for G and J as the $\varphi_x^j(y)$ are known (knowing $V(x, y)$). This leaves a time evolution equation for $\phi_{y_a}(x, t)$ that will be the master equation of (Alg.B):

$$i\hbar \frac{\partial \phi_{y_a}(x, t)}{\partial t} = \left\{ \left(-\frac{\hbar^2}{2m_x} \frac{\partial^2}{\partial x^2} + V(x; y_a(t)) \right) + \sum_{j=0}^{\infty} \left[U^j(x, t) \left(-\frac{\hbar^2}{2m_y} \frac{\partial^2}{\partial y^2} \varphi_x^j(y) \Big|_{y_a(t)} + i \frac{dy_a(t)}{dt} \frac{\partial}{\partial y} \varphi_x^j(y) \right) \right] \right\} \phi_{y_a}(x, t)$$

Which is now linear (even if non-unitary). For each time iteration, every term is known if we also evolve in a coupled fashion the equation for $\phi_{x_a}(y, t)$. Its equation will be the same as the above DE just flipping the variables and acknowledging that the adiabatic states for sections in y , $\varphi_y^j(x)$, will not in general be equal to those in x . The whole Born-Huang development would be the same otherwise.

This pair of equations can be evolved using a 1D CN algorithm, with the added details that: the potential energy will be complex and that even if $V(x, y)$ is time independent, the propagator matrices U_L and U_R will need to be updated in each time iteration (G and iJ do vary in time). In any case, Alg.B continues to have a polynomial complexity as Alg.A! Besides, it must be noted that in a computational implementation, the number of used j must be finite, which will be the other big approximation. Still, one can estimate in each time if most of the significant coefficients are used, by looking at whether the value Λ (the somewhat χ_x^j “norm”) is close to its “correct” value 1. This idea allowed to design an algorithm in which the number of used χ_x^j is self-regulated. Inputting a tolerance, say 0.95, in each time iteration, only the coefficients to obtain a Λ norm of at least 0.95 are used.

3.3.4 Our Benchmark Problem

In order to qualify whether the algorithm captures more correlation than Alg.A, we will consider an easy problem, but where there is already a non-factorisability: The single slit diffraction.

In particular, in order to ease the treatment, we will only consider Alg.B for $\phi_{y_a}(x, t)$. The coupled y direction SPCWF $\phi_{x_a}(y, t)$ will simply be evolved using Alg.A (setting $G = J = 0$).

As this is the first analysis we are performing on this new algorithm, we will just focus our attention in the impingement of an initial wave-packet that comes from a wide free space onto a slit/tunnel. That is, our problem will be modeled by the potential:

$$V(x, y) = \begin{cases} \infty & \text{if } x > 0 \text{ and } \text{abs}(y) > d \\ 0.0 & \text{else} \end{cases}$$

This could model half way the single slit diffraction or an electron on a path suddenly passing to a thinner channel. The point is that the entrance in the slit is the most critical part for a time evolution. The exit is trivial, but in the entrance geometrical correlations provoke a virtual barrier for impinging packets with less energy than the first resonant state energy of the tunnel (as we proved in the previous Section). This entanglement in principle should be impossible to be captured by the Alg.A that sets

$G=0$ (as it is due entirely to G) and thus supposes a perfect initial benchmark for the new algorithm.

It should be noted that in reality, the potential energy we will be dealing with, is not strictly the previously showed ideal one. Instead, in order to reduce numerical aberrations, the sudden increase to infinite potential in the y direction will be smoothed by a steep Gaussian increase. Also, typical wave reflections occur in the boundaries of the grid (no absorbing boundaries still implemented here). Thus, the boundaries of the grid behave as infinite potential walls as well. Still, the essence of the discussion is the same.

Actually, thanks to the boundaries acting as infinite potential walls, the adiabatic treatment turns out to be truly simple. The states $\varphi_x^j(y)$ will be the ones of the 1D particle in a box of length $L(x)$, as explained in Section 3.3.2. In this case:

$$L(x) = \begin{cases} y_{max} - y_{min} & \text{if } x < 0 \\ 2d & \text{else} \end{cases}$$

with y_{min} , y_{max} the considered boundaries of the grid in the y direction. The first and second derivatives of such sinusoidal adiabatic states (necessary for [Alg.B](#)) can analytically be obtained.

3.3.5 Testing $\chi^j(x, t)$ Quality

Once the potential and the adiabatic states are known, we are in the right paradigm to chose an initial wave-function and execute [Alg.B](#). For a first approach we will choose a 2D Gaussian ([2DG](#)) with $\sigma_x = 1.0$, $\sigma_y = 2.0$, $\mu_x = -6.0$, $\mu_y = 0.0$, $k_x = 1.0$.

The first test will be to check whether the coefficients χ^j of the Born-Huang expansion (the only approximated terms in the time evolution) remain around the “true” numerical values in a problem where they are really an approximation, like the Benchmark Problem. For a reference of the “true” values we will simultaneously evolve the full wave-function using the CN approach and we will calculate the coefficients $\chi^j(x, t)$ at each spatial point x and time. We will study then the evolution of the complex modulus of the $\chi^j(x, t)$ per j , per x and t (remember that they are complex coefficients). We will vary $2d$, the slit width from 14.0 to 4.0 and check the evolution of the $\chi^j(x, t)$ coefficients and the difference with respect to the reference CN. Due to the visual concordance, it was decided that using 4 representative trajectories that get to cross the entrance of the tunnel would be enough.

The analysis once again is full of multidimensional temporal data, which is hard to imprint in few static images. A view of the programmed χ_x^j monitoring environment can be seen in Figures 10 and 11 (for [Alg.B](#) and CN). Full animations of every studied case can be found in the work’s [repository](#).

Note that the χ_x^j with even j are almost zero in magnitude for all times and all points in x , as they are the projection coefficients onto antisymmetric adiabatic states: in these simulations the wave-function happens to be a symmetric wave-packet with respect to the plane $x = 0$. Therefore, whenever we say that 3 states were necessary for $\Lambda > 0.95$, in reality only $j = 1$ and $j = 3$ had non null coefficients (we omit $j = 0$ as its eigenstate is $\varphi_x^0(y) = 0$). This way, requiring 5 states is actually meaning that only the χ_j with $j = 1, 3, 5$ were significantly different from zero.

Each of the χ_x^j are both spatially and temporally varying coefficients, apart from being complex valued. As such, the best way to compare them is by observing the $|\chi_x^j|$ charts of CN and [Alg.B](#) animated in space and time. In any case, as a first naive study, attending together the norm Λ (which is only temporally varying) and the required number of χ_x^j -s to achieve the tolerance 0.95, it could be enough to capture the information of the approximated coefficients in a global perspective. These are collected in Table 2.

It can be seen both in the simulations and in the data in Table 2 that there is always an abrupt change in the number of χ^j just in the moment of the entrance, which then stabilizes generally to smaller values. For tunnel lengths ≥ 10 it seems that the chi evolution is neatly captured. However, the quality starts to decay rapidly, until at $2d = 6$ crazy χ^j numbers are required for the tolerance compared with CN. For $2d = 4$ the algorithm is unable to capture the χ^j evolution properly.

Table 2: Parameters abstracted from the simulations for the χ_x^j approximation quality test: Section 3.3.5. Everything in atomic units (a.u.)

Slit Length $2d$ Outside-Entrance-Inside the Slit		14.0 O E I	10.0 O E I	8.0 O E I	6.0 O E I	4.0 O E I	
Required number of χ_x^j for $\Lambda > 0.95$	CN		3 3 3	3 3 3	3 3 3	3 5 5	3 7 7
	Alg.B	Traj.1	3 3 3	3 5 3	3 13 11	3 15 +30	3 +30
		Traj.2	3 3 3	3 5 3	3 11 9	3 18 +30	3 +30
		Traj.3	3 3 3	3 5 5	3 11 7	3 27 +30	3 +30
		Traj.4	3 3 3	3 5 3	3 13 9	3 13 +30	3 +30
Λ when number of χ_x^j stabilized inside tunnel	CN		0.99	0.98	0.95	0.97	0.98
	Alg.B	Traj.1	0.99	0.95	0.95	0.91	0.80
		Traj.2	0.98	0.95	0.95	0.91	0.85
		Traj.3	0.99	0.97	0.95	0.90	0.85
		Traj.4	0.99	0.96	0.95	0.93	0.80

Two remarks should be considered at this point though. First, Alg.B evolves SPCWF-s, which in general have little to do with the full wave-function, which means that the χ_j coefficients for individual trajectories should not be expected to exactly coincide with the CN χ_x^j (related to the full wave-function). Rather a holistic view of the trajectory ensemble should be attended (as we will proceed to check now). Second, higher j coefficients contribute each time less to the Λ norm (see Figure 11), which means that in order to achieve only a bit more Λ , lots of states more need to be considered. That is why the number of required χ_j seems to grow that much. Thus, one would think that a better comparison could be achieved by directly analyzing j -wise the difference of the complex space-time profiles of χ_j . The point is that its representation happens to be problematic, as the CN algorithm uses a lighter grid than Alg.B and due to the dimensionality of the data (-space-time and complex plane- plus the different j). Thus a deeper analysis in the χ_j convergence matter is left for future works.

3.3.6 Testing if Correlations are Captured

Once we have checked that the χ^j , at least for certain regimes, are reasonably well approximated, we now want to check whether the geometrical correlations that should be hidden in G and J are correctly captured by the new algorithm. In particular we will use the fact that the apparently open entrance shows a virtual potential wall for impinging packets exclusively due to the entanglement between the degrees of freedom (correlation in G). Packets with less energy than the lowest resonant energy of the tunnel's x section, should be reflected from the open entrance, even if there is strictly no potential there. These resonant energies are approximately the energies of a particle in a box of length $2d$, as we proved in Section 3.3.3. Therefore, if the impinging packet has an energy lower than $E_1 = \frac{\pi^2 \hbar^2}{2m_x 4d^2}$, most of the probability density (most of the Bohmian trajectories) should be reflected. For sure, due to quantum tunneling, some of the probability will still cross the entrance, but it should be minimal.

At this point there is a little problem with the 2D Gaussian wave-packet with momentum $k_y = 0$ and varying k_x . It turns out that a quantum free particle ($V = 0$) does not only posses energy due to the kinetic energy ($\frac{\hbar^2 k^2}{2m}$). As we explained in Section 1, there is always present another energetic contribution due to the shape of the probability density: the quantum potential energy Q . This acts like an internal pressure that provokes the energy of the wave-packet being non-zero even if $k_x = 0$. In order to measure the energies of custom wave-packets, the mean energy was calculated using:

$$E_{wavePacket} = \frac{\langle \psi_{wp} | H | \psi_{wp} \rangle}{\langle \psi_{wp} | \psi_{wp} \rangle}$$

where the Hamiltonian H was approximated numerically acknowledging that it is hidden in the propagators U_L and U_R of the CN method as:

$$H \simeq \frac{2\hbar}{i\Delta t}(U_L - Id)$$

For the 2D Gaussian (2DG) in $V = 0$ with $\sigma_y = 2.0$, $\sigma_x = 1.0$ the energies of the wave-packet as a function of its k_x can be found in Table 3. Clearly only at high k_x its energy matches the semi-classically expected $\frac{\hbar^2 k_x^2}{2m}$. The problem with this is that we want to vary the k_x (the energy) of the packet ranging from smaller energies than the lowest resonant state of the tunnel to higher energies. It turns out that the described 2D Gaussian does not allow this in a reasonable regime of slit lengths 2d. In order to make the quantum potential energy lower, we could set $\sigma_x = 2.0$, but even still the energies were not found to be satisfactorily small. The next simplest decision was to design a wave-packet that would be Gaussian in the impinging x direction and the first adiabatic state (half a sine) in the y direction. This could even aid the algorithm to require less χ_x^j (even if this should not be the limiting point, as we already tested their consistency). The new wave-packet will be:

$$\psi(x, y, t = t_0) = \frac{1}{\sqrt[4]{2\pi\sigma_x^2}} e^{ik_x x - \frac{(x-\mu_x)^2}{4\sigma_x^2}} \sqrt{\frac{1}{a}} \sin\left(\frac{\pi(y+a)}{2a}\right)$$

with $a = 10$, $\sigma_x = 2.0$ and $\mu_x = -8.0$. Its calculated energies as a function of k_x can be found as well in Table 3.

Table 3: Energy of the initial wavepackets as a function of their initial momentum in x k_x ($k_y = 0$). Contrasted with the energy of a free particle if it only had kinetic energy. Everything in atomic units (a.u.)

k_x	0	0.15	0.25	0.35	0.55	0.65	0.75	0.95
$KE = \frac{\hbar^2 k_x^2}{2m}$	0	0.011	0.031	0.061	0.151	0.211	0.281	0.451
Energy GaussxGauss	0.156	0.167	0.187	0.218	0.308	0.370	0.437	0.607
Energy GaussxSin	0.043	0.055	0.075	0.105	0.195	0.255	0.325	0.495

It is unfortunate that not even with this packet, we can test the reflection at slits with $2d \sim 12$, where we got the greatest χ_x^j convergence. Anyhow, we can try it for $2d = 8$, 6 and 4 and this way even test the limits of the algorithm. Sure, we found that $2d = 4$ and $2d = 6$ cases were in the *crazy* χ_x^j regime, such that individual trajectories cannot be assured to be correct. However, let us test if an ensemble measurement changes this. We will set a high number of trajectories as to be able to approximate the probability density time evolution ($M = 150$) and vary the initial k_x to give the packet energies that are smaller, comparable and higher than the virtual wall (see Table 4). The test we will perform will be double edged, and quite demanding. On the one hand, we will compare the transmitted percentage of trajectories obtained using the new Alg.B, with the trajectory percentage and the probability density obtained using the more “exact” CN. This will be in order to check that the algorithm performs an approximately correct ensemble evolution. On the other hand, we will contrast it with the trajectory proportions transmitted using Alg.A, which is expected to be completely blind towards this correlation wall of the entrance (as it approximates $G=0$).

We can find all the heavy animations in the [repository](#). The absolute differences as a function of time between the algorithms are plotted in Figures 12 and 13. But their relevant data for the discussion is summarized in Table 4. The following observations can be abstracted:

- On the one hand, the simulations appear to show what we were looking for: for initial k_x such that the wave-packets should be reflected ($E_{wavepacket} - E_{Barrier1^{st}lvl} < 0$ in Table 4), only the CN and Alg.B seem to feel the presence of the wall: the probability densities in x direction, seem to collide with something at $x = 0$. On the contrary, the probability density of the SPCWF in x in Alg.A is fully blind with the presence of the virtual barrier, and it crosses with no collision.
- Attending the data in Table 4 our goal seems to be satisfied. Both for $2d = 8$ and $2d = 6$, the absolute differences of the final transmission (passed the impact) for CN and Alg.B happen to match very well. Way better than Alg.A with any of both. Actually, once again, the trajectories of Alg.B seem to even approximate better the probability density of CN, than the trajectories obtained from

the same CN density! This is probably due to the fact that being [Alg.B](#) polynomial in complexity, it allows a finner grid, which in turn makes the trajectories more sensitive. Also, attending the big differences with respect to CN between [Alg.B](#) and [Alg.A](#), the latter is very far from the dim transmission for forbidden entrance k_x . Thus the effect of the approximated G_a and J_a can be distinguished and the sought correlation seems to be captured.

- What is more, attending the maximum differences in time recorded during the evolution (which is even more demanding!) at $2d = 6$ and 8 , the better match of [Alg.B](#) with CN can be clearly seen. In general a feeling of how small the errors for [Alg.B](#) are, can be seen in Figure 12.
- In the $2d = 4$ case, for impinging energies smaller than the wall energy, [Alg.B](#) seems to match way better the CN evolution than [Alg.A](#). In fact, once again it can clearly be seen that [Alg.A](#) is blind with respect to the wall. Nonetheless, there is a little drawback: for bigger energies than the wall, there seems to be a change! Now [Alg.B](#) seems to be overestimating the wall and its transmittance is way lower than it should be! Making the introduction of the approximated G and J bad in this case. See the arrows in Figure 13: the errors of [Alg.B](#) compared with CN blast for higher k_x than the wall energy. Meanwhile, the errors for [Alg.A](#) stay relatively bounded.

Table 4: Parameters abstracted from the simulations for the analysis in the Transmitted Trajectory/Probability test: Section 3.3.6. Everything in atomic units (a.u.)

Slit length $2d$ Barrier 1 st lvl Energy			2d = 8 0.077				2d = 6 0.137				2d = 4 0.308				
		k_x $E_{wavepacket} - E_{Barreira1^{st}lvl}$	0.1 -0.028	0.17 -0.019	0.23 -7e-3	0.3 0.012	0.15 -0.082	0.25 -0.062	0.35 -0.032	0.65 0.118	0.35 -0.203	0.55 -0.113	0.75 0.017	0.95 0.187	
Transmitted Probability/Trajectory Proportion into the tunnel	Max. Abs. Difference in time	Alg.B with	CN Trajs	0.027	0.027	0.04	0.067	0.02	0.0134	0.0467	0.0533	0.0134	0.04	0.16	0.28
		Alg.A with	CN Prob. Density	0.0092	0.034	0.041	0.039	0.0062	0.0095	0.026	0.071	0.026	0.036	0.135	0.261
		Alg.B with	Alg.A Trajs	0.027	0.027	0.027	0.027	0.027	0.053	0.073	0.107	0.1067	0.093	0.147	0.193
	Values when Stabilized		CN Trajs	0.053	0.04	0.06	0.073	0.04	0.047	0.034	0.1	0.093	0.067	0.0467	0.0867
		Alg.A with	CN Prob. Density	0.027	0.053	0.057	0.05	0.0268	0.0530	0.0489	0.0515	0.082	0.085	0.050	0.067
	Abs. Difference when Stabilized		Alg.B	0.073	0.133	0.18	0.23	0.040	0.073	0.113	0.307	0.02	0.1267	0.133	0.173
		Alg.B with	CN Prob Density	0.073	0.112	0.155	0.216	0.0398	0.0743	0.129	0.372	0.042	0.133	0.260	0.373
		Alg.A with	CN Trajs.	0.053	0.12	0.16	0.187	0.0267	0.0733	0.147	0.36	0.033	0.16	0.28	0.4
		Alg.B with	Alg.A	0.093	0.167	0.2	0.25	0.067	0.12	0.173	0.406	0.127	0.22	0.273	0.313
	Abs. Difference when Stabilized	Alg.B with	CN Prob. Density	0	0.021	0.025	0.014	2e-4	1.3e-3	0.016	0.065	0.022	6e-3	0.127	0.2
		Alg.A with	CN Trajs	0.02	0.013	0.02	0.043	0.0133	0	0.014	0.053	0.013	0.033	0.147	0.227
		Alg.B with	Alg.A Trajs	0.02	0.034	0.02	0.02	0.027	0.047	0.06	0.099	0.107	0.093	0.14	0.14
		Alg.A with	CN Prob. Density	0.02	0.034	0.045	0.02	0.027	0.0457	0.044	0.034	0.085	0.087	0.013	0.06
		Alg.B with	CN Trajs	0.04	0.047	0.04	0.063	0.04	0.047	0.026	0.046	0.094	0.06	7e-3	0.087

3.3.7 Conclusions of the Tests

When it comes to the prediction of the χ_x^j adiabatic coefficients, tunnels with $2d \sim 10$ appear to be captured very stably. However, the current implementation of the algorithm fails at $2d < 6$.

Attending the evolution of the probability densities, we have seen that while the tunnel does not get too narrow ($2d \geq 6$), the Kinetic-Advection approximation on G and J ([Alg.B](#)) seems to capture almost perfectly the time evolution of the ensemble. However, when the tunnel gets too narrow, apart from the χ_x^j convergence being unclear, the evolutions appears to over-estimate the correlation potential it should capture.

Therefore, more analysis and tests are a necessity in order to check whether the lack of convergence for narrow slits is due to the algorithm itself, or some aspect of the code implementation. An immediate improvement that should be checked would be to evolve also the SPCWF in x using [Alg.B](#) (as it is fundamental in the coupled evolution). Alternatively the mass of the packet could be varied seeking lower energy packages and clearer reflections.

Anyhow, as a first analysis of the algorithm, the improvement of [Alg.A](#), which had $G=J=0$, appears clear enough. Therefore, we conclude that the research direction is promising.

4 In a Nutshell

The readers who have dug into any of the first two sections, will have acknowledged how dramatic it is to predict the behavior of a quantum system with more than just a few particles. We have all the tools in our hands: all the necessary equations are clearly intuitive (Section 1) and we have the stablest of the methods to simulate those systems (Section 2). However, as understandable as these are, even in the generalized n dimensional form we arrived to derive in both sections, as soon as we begin to touch the gears of reality, we suddenly bump into an exponentially complicated wall, both in space and in time. The Universe has made a detailed prediction of her impossible in a human life-scale. Nature has definitively set there a human-proof lock.

However, anyone reading the third section will have noticed that we have been smart enough as to find ways to hack this lock around. It all has to do with sacrificing perfection. As it is said, “good enough is the enemy of perfection”. We presented a heavy machinery based on Bohmian Mechanics that collected all the difficulties (entanglements, correlations) that were hidden in a quantum system in just two potential energy terms G and J . We showed a system of equations (**PSE**) where these two terms, the exact roots of the many body problem, surfaced explicitly. We could now directly attack the heart of the many body problem by trying to capture the biggest part of their essence (approximating them), but without sacrificing human time-scales (keeping calculations in a polynomial space and time)!

We first presented **Alg.A**, which kept only the zero-th order Taylor terms of G and J (which turned out to be $G=J=0$). We tested the algorithm in the 2D double slit experiment, which we had already studied using the “exacter” 2D Cranck Nicolson approach in section 2. We compared the interference patterns and transmission emerging in the simulations and found that **Alg.A** was capable of capturing their physics.

However, we then noticed that **Alg.A** was limited to the correlations present in the classical V potential. In particular, quantum subtleties as the “virtual” barrier emerging in a suddenly confined transport direction, are invisible for **Alg.A**. In the entrance of such a tunnel, the classical potential is null, but only the packets with energies bigger than the “virtual” resonance barrier are allowed to fully enter. In other words, if the packet has a smaller energy, it should be entirely reflected. With the motivation to capture this correlation, we presented **Alg.B**, where we arrived at more elaborated expressions for G and J introducing the Born-Huang expansion for the wave-function. We tested for the very first time the convergence of the main approximated elements in **Alg.B** (the χ_x^j coefficients of the (**BHE**)), centering our attention on the entrance of a packet in a confined tunnel. We found that for tunnel widths $2d > 8$ the χ_x^j were approximated very stably by **Alg.B**. Finally, we proceeded to check whether the correlation that **Alg.A** failed to capture was now grasped: we measured the transmittance of the trajectories for varying initial packet energies for several different slit widths. We conducted simulations in these same conditions using CN and **Alg.A**. Effectively, we found that **Alg.B** and CN captured this barrier in the entrance (making their transmittances small when the impinging packet’s energy was small), while **Alg.A** was blind and had a high transmission for any initial packet energy. With this, we concluded a first naive analysis for the new **Alg.B**. and a more exhaustive analysis was left for future works.

With this, we hope that the reader has been convinced that the many body problem is a true problem, but not a failed battle. Even today there are still many unexplored mathematical frameworks, that will one day allow us dodge the exponential wall and give us the power to weave ourselves the underlying fabric of reality.

Supplementary Figures

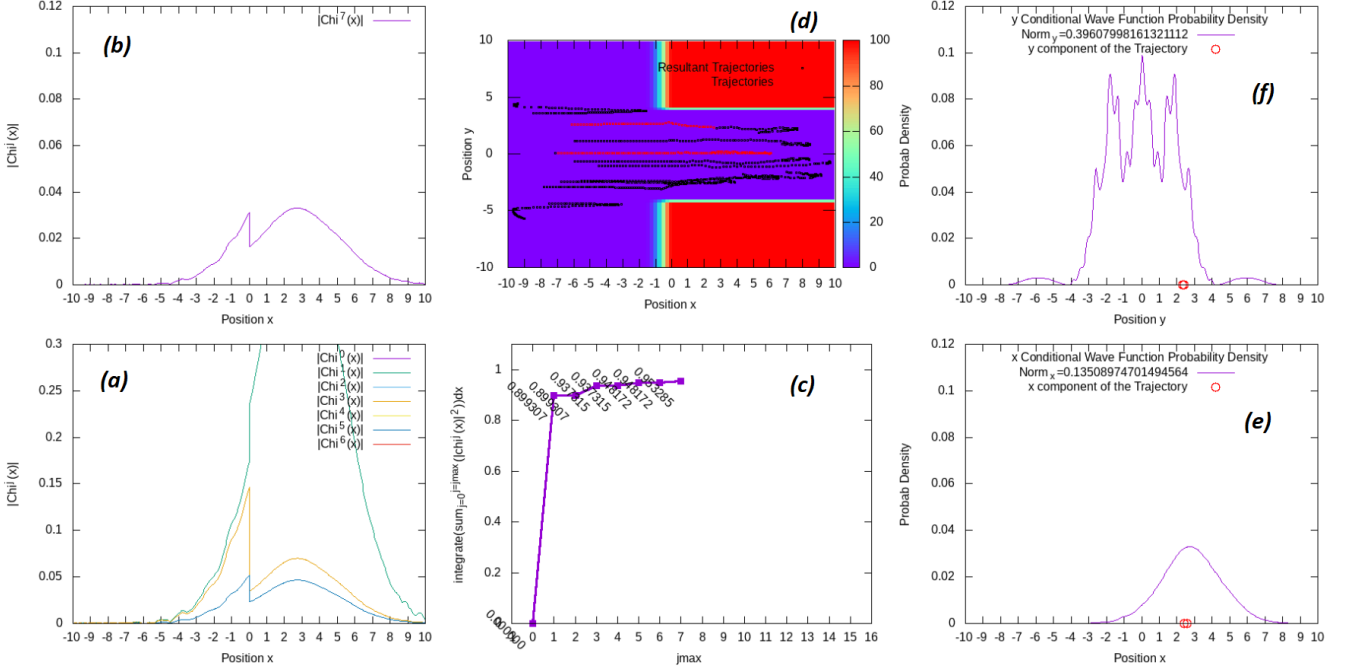


Figure 10: A view of the Evolver of *Alg.B* and the χ_j coefficient monitoring environment programmed ad hoc. The χ_j are ones approximated and actively used in *Alg.B*. In (a) the $\chi_j(x,t)$ profiles of the first half of the used coefficients are animated. In (b) the second half. Note the scale difference. In (c) for the used $\chi_j(x,t)$ (such that $\Lambda < \text{tol}$), the value of Λ if the number of $\chi_j(x,t)$ was truncated at the j -th is plotted. See how the higher j contribute each time less to Λ . In (d) the evolved trajectories in black (the active animated ones in red) and the potential profile color mapped. In (e) the probability density of the x -SPCWF $\Phi_x(x,t)$, in (f) the one for the y -SPCWF $\Phi_y(y,t)$.

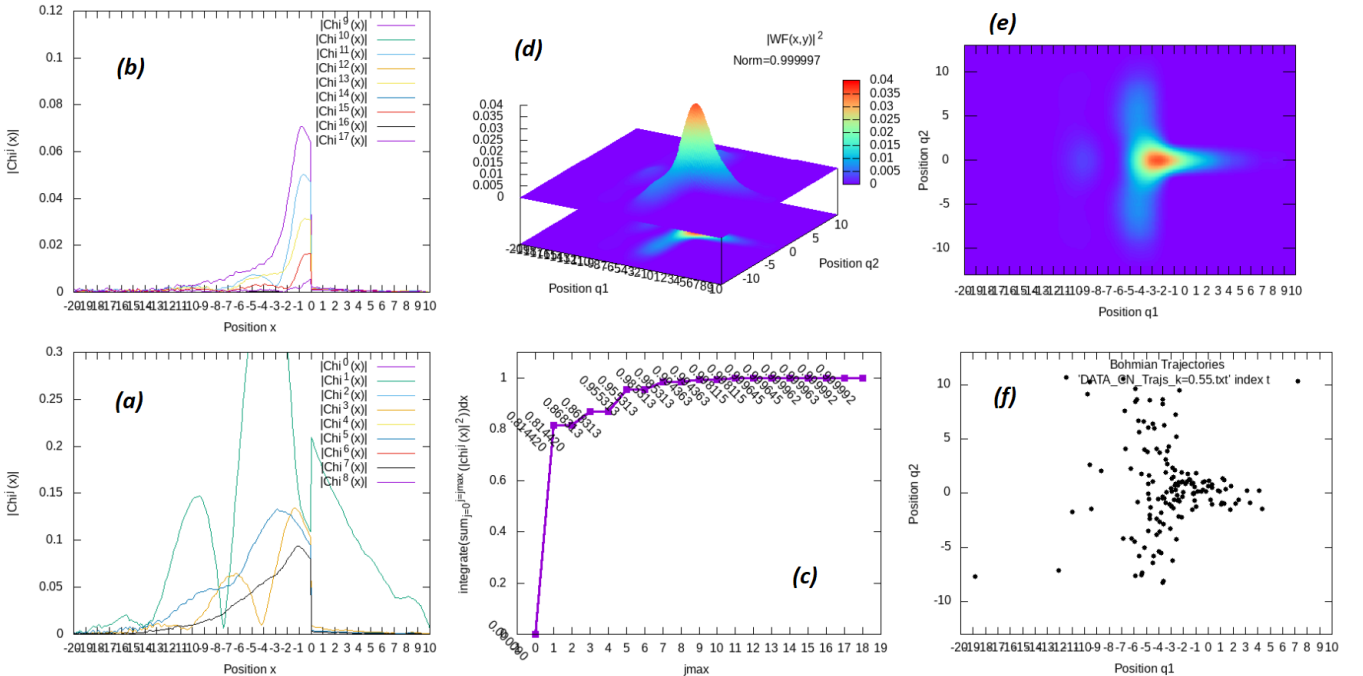
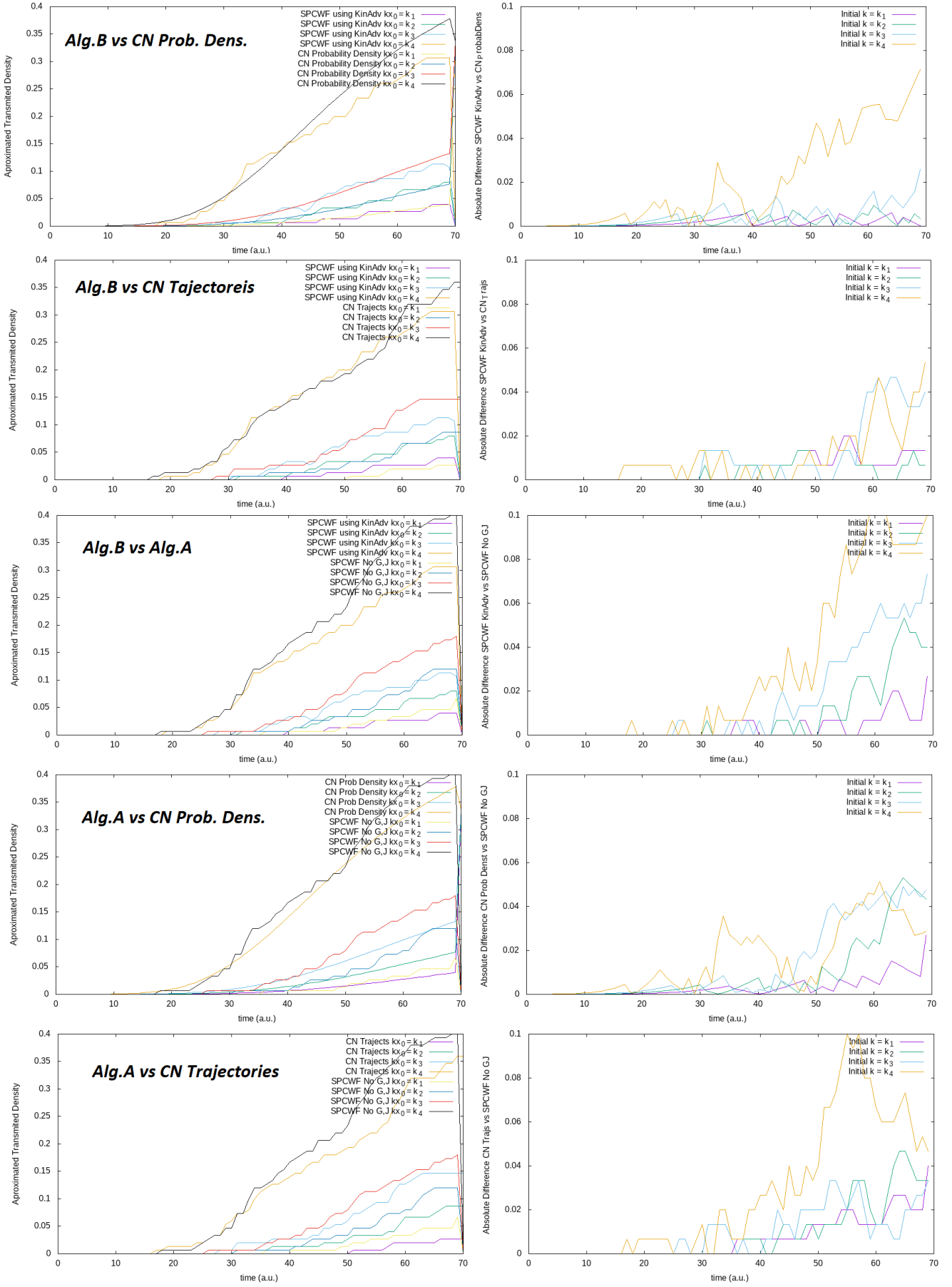


Figure 11: A view of the Crank-Nicolson evolver and χ_j coefficient monitoring environment designed ad hoc. The χ_j are calculated *a posteriori* from the “exact” full-wavefunction. In (a) the $\chi_j(x,t)$ profiles of the first half of the maximum allowed coefficients are animated. In (b) the second half. Note the scale difference. In (c) the value of Λ if the number of $\chi_j(x,t)$ was truncated at the j -th is plotted. See how the higher j contribute each time less to Λ . The plots seem similar to those in Figure 10, but the computation here is “exact” using a full CN wave-function while in the other they are approximated using *Alg.B*’s SPCWF-s. In (d) a 3D map of the probability density of the full-wavefunction (in x, y) and in (e) its color map. In (f) some Bohmian Trajectories are animated for visual check of the congruence.



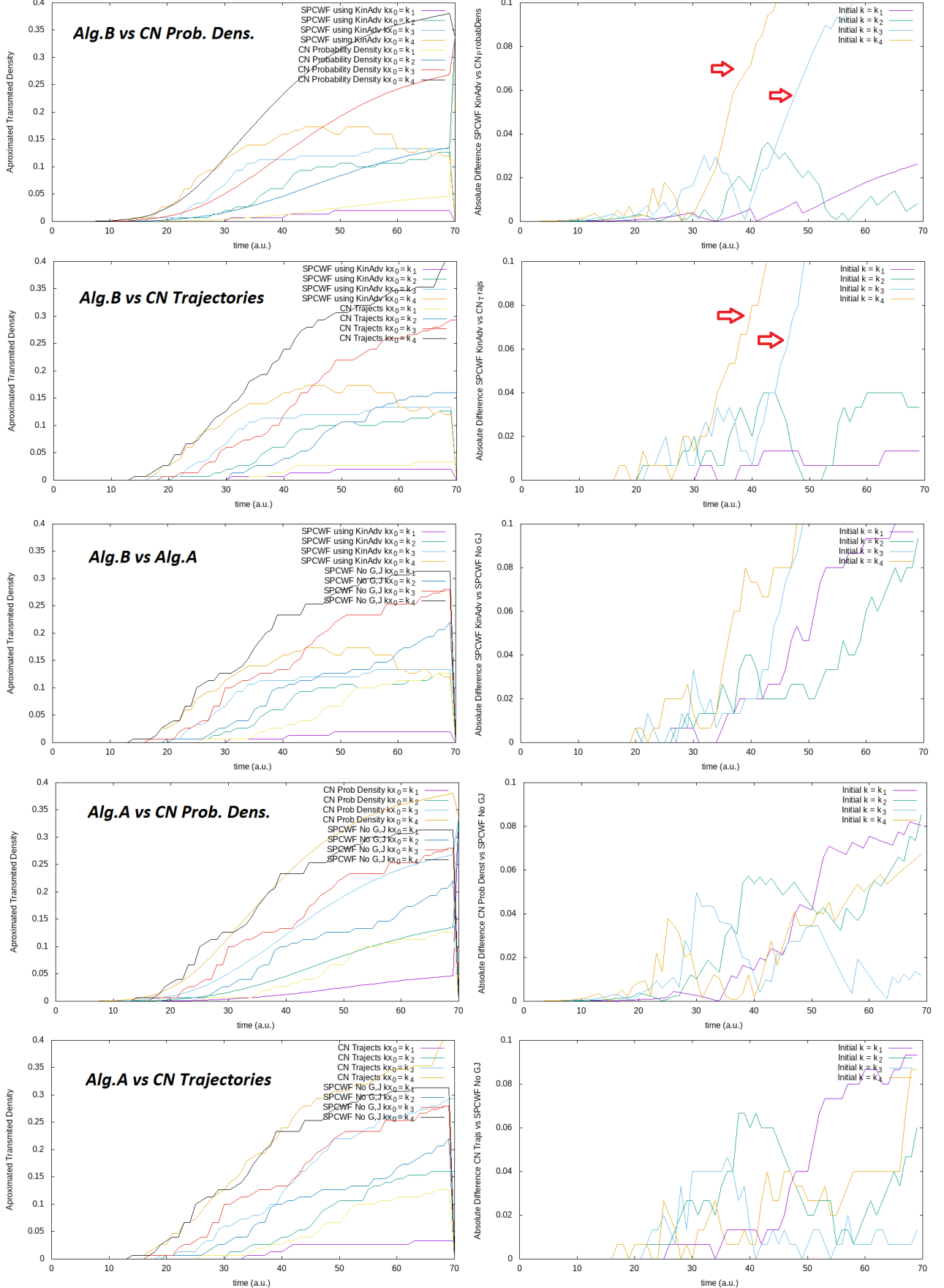


Figure 13: Using $2d = 4$ and 150 trajectories, these are the transmittances in time (left) and the absolute differences (right) obtained using the different algorithms (see legends -KinAdv means Alg.B-). Note how Alg.B now performs worse than Alg.A for high k (k_3 and k_4). The values of k are listed in 6. The parameters used here are the ones used in Table 4. Note how even if for small k the Alg.B matches very well CN (first two images), for bigger k errors blast (arrows). An inverse trend appears for Alg.A (last two).

Acknowledgments

The work on Algorithm B ([Alg.B](#)) was done under the research project **QUANTUM CAT**, by the Catalan Government: “*AGRUPACIÓ EMERGENT EN TECNOLOGIES QUÀNTIQUES DE CATALUNYA (QUANTUM CAT)*”; 001-P-001644; Active from 01/01/2018 till 31/12/2020;

Subproject: “*QUASIBOHM*” (*UAB*) MAIN RESEARCHER: Xavier Oriols;

APPENDIXES

Appendix A: Grid Parameters for the Simulations of the Figures

Table 5: Numerical Grid Parameters for the generation of animations in the Figures. For every of them: $t_0 = 0.0$, $m_k = 1.0$ and $\hbar = 1.0$. J_i stands for the number of intervals of the grid in coordinate i , j_{max} and j_{min} for the grid limits. j_{max} stands for the maximally allowed dynamically adjusted number of χ_j coefficients.

Figure-Animation of Figure	Num. of Time Iterations	Δt	J_x	xmin	xmax	J_y	ymin	ymax	Num. of Trajectories	j_{max}	Λ Tolerance
Figure 1	1000	0.01	1000	-6.0	6.0				60		
Figure 2	1000	0.01	1000	-5.0	5.0				60		
Figure 4	340	0.005	1000	-6.0	8.0				120		
Figure 5	340	0.005	1000	-6.0	8.0				120-60		
Figures 6 and 7	1500	0.004	260	-15.0	20.0	260	-15.0	15.0	150		
Figure 8	1500	0.004	850	-15.0	20.0	730	-15.0	15.0	350		
Figure 9	1500	0.004	850	-15.0	20.0	730	-15.0	15.0	150		
Table 2	14000	0.001	700	15.0	20.0	600	-11.0	11.0	25	35	0.95
Table 4 CN	4200	0.004	750	-20.0	10.0	600	-13.0	13.0	150	20	0.95
Table 4 Alg.A and Alg.B	4200	0.004	340	-20.0	10.0	240	-13.0	13.0	150	20	0.95
Figure 14 and 15	3000	0.005	2000	-8.0	8.0				120		
Figrule 16	1500	0.01	250	-8.0	8.0	250	-8.0	8.0			

Table 6: Numerical values of k_i used in the Figures.

Figure-Animation of Figure	k_1	k_2	k_3	k_4	k_5	k_6	k_7	k_8	k_9	k_0
Figure 5	1.5	2.5	3.5	4.5	5.5	6.5	7.5	8.5	9.5	0.5
Figure 7	2.0	4.0	6.0							
Figure 9	2.0	4.0	6.0							
Figure 12	0.15	0.25	0.35	0.65						
Figure 13	0.35	0.55	0.75	0.95						

Appendix B: Imaginary Time Evolution

The following is a very practical numerical technique to find the ground state and some of the excited states of a quantum system using a numerical SE time evolver. The theoretical grounds are very interesting and straight-forward:

Given an n dimensional quantum system and its Hamiltonian \hat{H} (that will be assumed to be time independent), we will denote its eigenstates by $\{\phi_n(\vec{q})\}_{n=0}^{\infty}$ and their corresponding eigenvalues $\{E_n\}_{n=0}^{\infty}$ which are real and ordered, being E_0 the smallest. Any acceptable wave-vector ψ can be expressed as a linear combination of the stationary states of this system $\{\phi_n\}_n$. This is because they are the eigenstates of a Hermitian operator, by which they form an orthonormal basis of the State Space. That is $\exists c_n \in \mathbb{C}$ s.t.:

$$\psi(\vec{q}, t_0) = \sum_{n=0}^{\infty} c_n \phi_n(\vec{q})$$

The SE time evolution of this initial wave-vector will be, as exposed in Section 2:

$$\psi(\vec{q}, t) = e^{-\frac{i}{\hbar} \hat{H}t} \psi(\vec{q}, t_0) = e^{-\frac{i}{\hbar} \hat{H}t} \sum_{n=0}^{\infty} c_n \phi_n(\vec{q})$$

Where applying the fact that ϕ_n are the eigenstates of \hat{H} :

$$\psi(\vec{q}, t) = \sum_{n=0}^{\infty} c_n e^{-\frac{i}{\hbar} E_n t} \phi_n(\vec{q})$$

This way we have the time evolution of the wave-function expressed as the time evolution of some complex coefficients $\eta_n(t) = c_n e^{-\frac{i}{\hbar} E_n t}$. Now, if we let us make the change $it \rightarrow \tau$ and consider τ as the new “real” time axis:

$$\psi(\vec{q}, t) = \sum_{n=0}^{\infty} c_n e^{-\frac{1}{\hbar} E_n t} \phi_n(\vec{q})$$

As time τ increases, this describes an exponential decay of each of the projection coefficients c_n of the initial vector in each eigenstate. The point is that the decrease rate is proportional to the energy E_n of the eigenstate. Therefore, after a certain time, the higher energy state’s coefficients will become negligible and the remaining state will be proportional to the ground state of the Hamiltonian ϕ_0 . That is:

$$\lim_{\tau \rightarrow \infty} \psi(\vec{q}, \tau) \propto \phi_0(\vec{q})$$

This will happen regardless of the initial state $\psi(\vec{q}, t_0)$ as long as it has a non-zero projection in the ground state ($c_0 \neq 0$). If not, the wave-vector will tend to the lowest energy eigenstate with non null coefficient c_n . This by the way, is how one can obtain excited states using the present idea.

An important remark is that the evolution is non-unitary, and thus, the wave-function should be normalized at each time.

In practice this method can be programmed using for instance the already implemented CN, by simply changing every i for a 1.0 in the propagator matrices.

It would be certainly interesting to try to apply this idea to the approximated Alg.A and Alg.B, for an easy extraction of ground states of dimensionally hard systems (very interesting for quantum chemistry). The problem is that when erasing the complex unit i , velocity fields, which relied on the complex phase, disappear. Thus Alg.A and Alg.B, centered in the evolution of a trajectory, suddenly freeze. Paradoxically, the evolution becomes real. A solution for this is the following:

Dissipative Imaginary Time Evolution

Instead of changing $i \rightarrow 1$, if $i \rightarrow i \varepsilon_{SE} + \varepsilon_{Dis}$, now we would have control on the degree of dissipative evolution ε_{Dis} and the degree of Schrödinger evolution ε_{SE} :

$$\psi(\vec{q}, t) = \sum_{n=0}^{\infty} c_n e^{-i \frac{E_n}{\hbar} \varepsilon_{SE} t} e^{-\frac{E_n}{\hbar} \varepsilon_{Dis} t} \phi_n(\vec{q})$$

If $\varepsilon_{Dis} = 0$ and $\varepsilon_{SE} = 1$ we recover a normal SE evolution, but if $\varepsilon_{Dis} = 1$ and $\varepsilon_{SE} = 0$ we have a pure imaginary time evolution. The point is that, for instance $i \rightarrow i + 1$ would yield mixed dynamics.

On the one hand, the state vector would go on trying to evolve according to the SE, but at the same time there would be a leakage of the higher energy components. Thus, if normalized at each time, this could be seen as a Schrödinger evolution with a sort of friction or energy dissipation. Therefore, this mixed evolution does allow the computation of velocity fields and trajectories, and thus an exploration of [Alg.A](#) and [Alg.B](#) in this direction.

In particular, all of this was can be implemented such that the parameters ε can be scheduled to take specific values at certain times. This is interesting for instance, for the simulation of the cooling preparation of an initial state for Bose Einstein Condensate experiments. If for example, we are interested on beginning our simulations using the ground state of the hydrogen atom in a different potential, we could set a time dependent potential, such that for a short preparation time, the potential is the Hydrogen Coulomb potential and $i \rightarrow 1$, and once we have acceptably obtained the ground state we switch off the dissipation $i \rightarrow i$ and the potential changes in step to the system we want to analyze.

The affordability of this approach on [Alg.A](#) and [Alg.B](#) will be explored in future works, for now, we have implemented it using CN. We can see for instance in Figure 14 how beginning the evolution with a symmetric state (a cosine) imaginary time evolution gives us the familiar Gaussian ground state in a harmonic 1D potential. Meanwhile, beginning with an antisymmetric state like a sine (Figure 15), we obtain the first eigenstate (as the projection in even states is null). At this point, we could subtract the state of this time to the dissipating wave-function, and we would erase the influence of the first eigenstate, thus allowing the emergence of higher energy states as well. In the animation [repository](#) you can find what it looks like the mixed dissipative dynamics, where trajectories are also evolved. You can check several different values for $\varepsilon_{SE} + \varepsilon_{Dis}$.

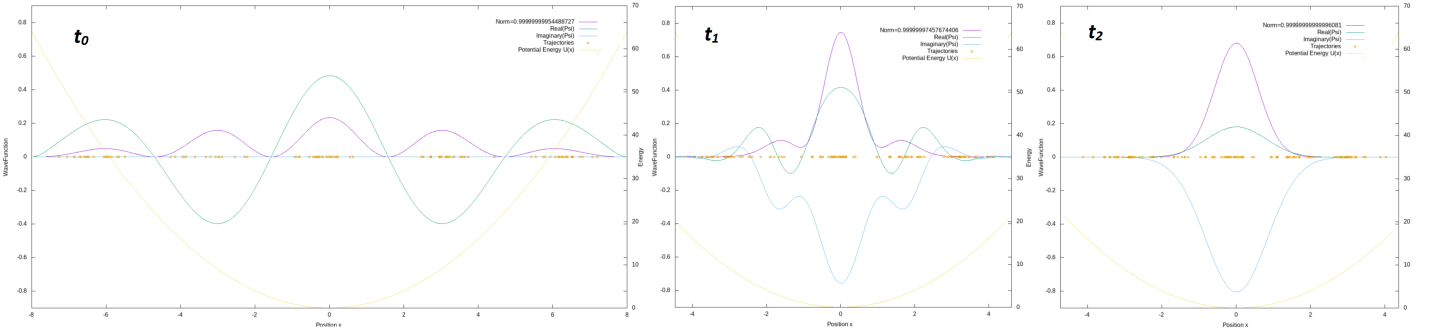


Figure 14: From left to right increasing time instances of a mixed dissipative time evolution using $i \rightarrow 0.1 + i$ in a harmonic well. Initially the wavefunciton is a cosine: we get the ground state of the harmonic well.

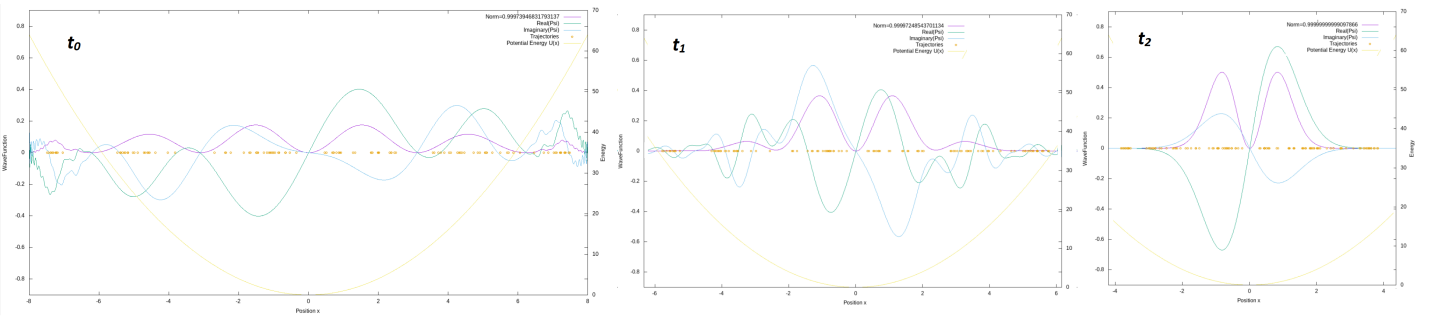


Figure 15: From left to right increasing time instances of a mixed dissipative time evolution using $i \rightarrow 0.1 + i$ in a harmonic well. Initially the wavefunciton is a sine: we get the first excited state.

In Figure 16 we put a 2D Gaussian at some point of a Toroidal potential (a spherically symmetric “donut” harmonic potential). We can clearly see how the achieved state is the expected Gaussian torus. In the [repository](#) you can check the beautiful motion the Gaussian does if we turn off dissipation.

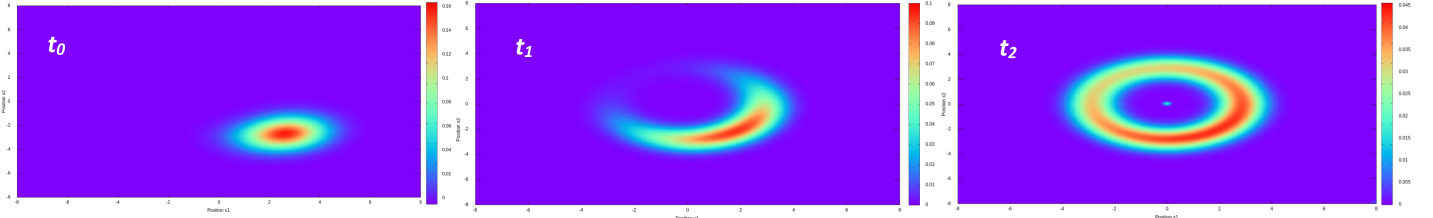


Figure 16: A 2D Gaussian in a Toroidal Potential Evolved using purely imaginary time evolution $i \rightarrow 1$. From left to right different snapshots of the time evolution of the probability density.

Appendix C: Important Properties of the Adiabatic Coefficients

Proposition 1. *The adiabatic states form an orthonormal basis in y :*

$$\int_{-\infty}^{\infty} \varphi_x^j(y)^\dagger \varphi_x^j(y) dy = \delta_{i,j}$$

Proof. The proof is immediate from the fact that they are the set of eigenvectors of a hermitian operator ($H_x(y)$ defined in 3.3.1). o.ε.δ

Proposition 2. *The adiabatic coefficients $\chi^j(x, t)$ can be obtained by:*

$$\chi^j(x, t) = \int \varphi_x^j(y)^\dagger \psi(x, y, t) dy$$

Proof. Introducing the Born-Huang expansion in the rhs and using the adiabatic state orthonormality with respect to the spatial coordinate y :

$$\int \varphi_x^j(y)^\dagger \psi(x, y, t) dy = \int \varphi_x^j(y)^\dagger \left(\sum_{k=0}^{\infty} \chi^k(x, t) \varphi_x^k(y) \right) dy = \sum_{k=0}^{\infty} \chi^k(x, t) \int \varphi_x^j(y)^\dagger \varphi_x^k(y) dy = \chi^j(x, t)$$

o.ε.δ

Proposition 3. *If we define the quantity Λ as:*

$$\Lambda := \sum_{j=0}^{\infty} \int_{-\infty}^{\infty} |\chi^j(x, t)|^2 dx$$

Then adiabatic coefficients $\chi^j(x, t)$ satisfy the normalization condition given by $\Lambda = 1$.

Proof. Using the normalization of the full wavefunction $\Psi(x, y, t)$ and the adiabatic state orthonormality the proof is straightforward:

$$\begin{aligned} \iint |\psi(x, y, t)|^2 dx dy &= \iint \psi(x, y, t)^\dagger \psi(x, y, t) dx dy = \iint \left(\sum_{k=0}^{\infty} \chi^k(x, t) \varphi_x^k(y) \right)^\dagger \left(\sum_{j=0}^{\infty} \chi^j(x, t) \varphi_x^j(y) \right) dx dy = \\ &\iint \sum_{k, j=0}^{\infty} \varphi_x^k(y)^\dagger \chi^j(x, t)^\dagger \chi^k(x, t) \varphi_x^j(y) dx dy = \int \sum_{k, j=0}^{\infty} \chi^k(x, t)^\dagger \left(\int \varphi_x^k(y)^\dagger \varphi_x^j(y) dy \right) \chi^j(x, t) dx = \\ &= \sum_{k, j=0}^{\infty} \int \chi^j(x, t)^\dagger \chi^j(x, t) dx = \sum_{j=0}^{\infty} \int_{-\infty}^{\infty} |\chi^j(x, t)|^2 dx \end{aligned}$$

Noting that $\iint |\psi(x, y, t)|^2 dx dy = 1 \ \forall t$, due to the SE causing a unitary evolution, the proof is completed. o.ε.δ

Appendix D: The Laplacian

Given $\rho(q_1, \dots, q_n) = \rho(\vec{q})$ is a scalar field $\rho : \mathbb{R}^n \rightarrow \mathbb{R}$, we define the Laplacian of ρ as:

$$\text{Laplacian}(\rho) := \text{div}(\text{grad}(\rho)) = \vec{\nabla} \cdot (\vec{\nabla} \rho) \equiv \nabla^2 \rho$$

In Cartesian coordinates $\vec{\nabla} := (\frac{\partial}{\partial q_1}, \dots, \frac{\partial}{\partial q_n})$, which yields:

$$\nabla^2 \rho(\vec{q}) = \frac{\partial^2 \rho(\vec{q})}{\partial q_1^2} + \dots + \frac{\partial^2 \rho(\vec{q})}{\partial q_n^2}$$

Let us understand intuitively the information this new scalar field gives us about ρ , following an idea of Ref. [3]. Let $\rho(\vec{q})$ have the value $\rho_0 \in \mathbb{R}$ at a certain point of its support, which from now on will be taken as the origin of the Cartesian coordinate system (that is, now $\rho(\vec{0}) = \rho_0$). Consider a hypercube in \mathbb{R}^n of side a , centered in the origin. The average value of the field ρ in the hypercube will be obtained by adding up the value ρ takes in each point of the interior, divided by the volume of the cube:

$$\bar{\rho} = \frac{1}{a^n} \iint \cdots \iint_{-a/2}^{a/2} \rho(\vec{q}) dq_1 \cdots dq_n$$

In order to evaluate the integral, we will Taylor expand $\rho(\vec{q})$ centered at the cube's barycenter $\vec{q} = \vec{0}$:

$$\rho(\vec{q}) = \rho(\vec{0}) + \sum_k \frac{\partial \rho(\vec{q})}{\partial q_k} \Big|_{\vec{q}=\vec{0}} q_k + \frac{1}{2} \sum_k \sum_j \frac{\partial^2 \rho(\vec{q})}{\partial q_k \partial q_j} \Big|_{\vec{q}=\vec{0}} q_k q_j + \dots$$

If the side a of the hypercube is small enough ($a \ll$) we could truncate the series at second order and insert it into the integral of the mean value of ρ in the cube:

$$\bar{\rho} \simeq \frac{1}{a^n} \iint \cdots \iint_{-a/2}^{a/2} \left(\rho_0 + \sum_k \frac{\partial \rho(\vec{q})}{\partial q_k} \Big|_{\vec{q}=\vec{0}} q_k + \frac{1}{2} \sum_k \sum_j \frac{\partial^2 \rho(\vec{q})}{\partial q_k \partial q_j} \Big|_{\vec{q}=\vec{0}} q_k q_j \right) dq_1 \cdots dq_n$$

Noting that if c is a constant:

$$\int_{-a/2}^{a/2} c q_k dq_k = 0 \quad \forall c \in \mathbb{R}$$

$$\iint_{-a/2}^{a/2} c q_k q_j dq_k dq_j = \int_{-a/2}^{a/2} \left(\int_{-a/2}^{a/2} c q_k dq_k \right) q_j dq_j = 0 \quad \text{if } i \neq j$$

Only $q_k \cdot q_j$ terms with $k = j$ can be non-null. Actually, if we had truncated the series at third order, all the third order terms would be canceled as well: they always contain an odd function integrated in $(-a/2, a/2)$. Therefore, to third order, we have that the mean value of ρ in the cube will be:

$$\begin{aligned} \bar{\rho} &\simeq \frac{1}{a^n} \iint \cdots \iint_{-a/2}^{a/2} \left(\rho_0 + \frac{1}{2} \sum_k \frac{\partial^2 \rho(\vec{q})}{\partial q_k^2} \Big|_{\vec{q}=\vec{0}} q_k^2 \right) dq_1 \cdots dq_n = \frac{1}{a^n} \left(a^n \rho_0 + \frac{a^{n+2}}{24} \sum_k \frac{\partial^2 \rho(\vec{q})}{\partial q_k^2} \Big|_{\vec{q}=\vec{0}} \right) \\ \bar{\rho} &\simeq \rho_0 + \frac{a^2}{24} \nabla^2 \rho(\vec{q}) \Big|_{\vec{q}=\vec{0}} \end{aligned}$$

Therefore if $a \rightarrow 0$, up to third order:

$$\nabla^2 \rho(\vec{q}) \Big|_{\vec{q}=\vec{0}} \simeq \frac{24}{a^2} \left(\bar{\rho}_{\text{cube } a \text{ around } \vec{0}} - \rho(\vec{q} = \vec{0}) \right)$$

That is, the value of the Laplacian of a scalar field at a point is a measure of the difference between the average value of the field in a neighborhood of that point and the value of the field at the point itself. In other words, the value of ρ in each point \vec{q} differs from the average value in its locality by a proportional quantity to $\nabla^2 \rho(\vec{q})$. The bigger the mean local departure of the function around that point, the bigger in magnitude the Laplacian will be. If the value of ρ in the surrounding points as an average is smaller than in the point, the Laplacian at the point will be negative; else, it will be positive.

Appendix E: Derivation of the Conditional Pseudo Schrödinger Equations (PES)

Assuming the discussion of section 3.1. and following the development in Chp.1 V 6 of [1]: In order to find a Schrödinger like equation of motion for the SPCWF we are going to employ the following “trick”. An arbitrary single valued complex function $f(x, t) : \mathbb{R}^2 \rightarrow \mathbb{C}$ can be imposed to be the solution of a 1D Schrödinger equation:

$$i\hbar \frac{\partial f(x, t)}{\partial t} = -\frac{\hbar^2}{2m} \frac{\partial^2 f(x, t)}{\partial x^2} + W(x, t)f(x, t)$$

if the potential term $W(x, t)$ is defined as:

$$W(x, t) := \left(i\hbar \frac{\partial f(x, t)}{\partial t} + \frac{\hbar^2}{2m} \frac{\partial^2 f(x, t)}{\partial x^2} \right) \frac{1}{f(x, t)}$$

The proof is immediate. An observation that we must note is that for an arbitrary $f(x, t)$, the potential $W(x, t)$ can be complex as well! Which is not the case in the usual Schrödinger Equation.

Then, using this for the SPCWF Φ_a , we will obtain its one dimensional SE if we carefully evaluate it in polar form $\Phi_a = \mathbf{r}e^{i\mathcal{S}/\hbar}$, in the necessary expression for $W(q_a, t)$:

$$W(q_a, t) = \left(i\hbar \frac{\partial \Phi_a(q_a, t)}{\partial t} + \frac{\hbar^2}{2m_a} \frac{\partial^2 \Phi_a(q_a, t)}{\partial q_a^2} \right) \frac{1}{\Phi_a(q_a, t)} = \left(i\hbar \frac{\partial(\mathbf{r}e^{i\mathcal{S}/\hbar})}{\partial t} + \frac{\hbar^2}{2m_a} \frac{\partial^2(\mathbf{r}e^{i\mathcal{S}/\hbar})}{\partial q_a^2} \right) \frac{1}{\mathbf{r}e^{i\mathcal{S}/\hbar}}$$

using the Leibniz derivation rule several times and an inverse chain rule, rearranging we arrive at:

$$W(q_a, t) = -\frac{\partial \mathcal{S}_a}{\partial t} - \frac{1}{2m_a} \left(\left(\frac{\partial \mathcal{S}_a}{\partial q_a} \right)^2 - \frac{\hbar^2}{\mathbf{r}_a} \frac{\partial^2 \mathbf{r}_a}{\partial q_a^2} \right) + i \frac{\hbar}{\mathbf{r}_a^2} \left(\frac{\partial \mathbf{r}_a^2}{\partial t} + \frac{\partial}{\partial q_a} \left(\frac{\mathbf{r}_a^2}{m_a} \frac{\partial \mathcal{S}_a}{\partial q_a} \right) \right)$$

Separating the real and imaginary parts:

$$\text{Re}\{W(q_a, t)\} = -\frac{\partial \mathcal{S}_a(q_a, t)}{\partial t} - \frac{1}{2m_a} \left(\left(\frac{\partial \mathcal{S}_a}{\partial q_a} \right)^2 - \frac{\hbar^2}{\mathbf{r}_a} \frac{\partial^2 \mathbf{r}_a}{\partial q_a^2} \right)$$

Where we can recognize the QHJE for a single particle in 1D. As such, the real part of W is simply the scalar real potential, then the Hamiltonian, followed by the kinetic energy and the quantum potential of a 1D particle.

$$\text{Im}\{W(q_a, t)\} = \frac{\hbar}{\mathbf{r}_a(q_a, t)^2} \left(\frac{\partial \mathbf{r}_a^2}{\partial t} + \frac{\partial}{\partial q_a} \left(\frac{\mathbf{r}_a^2}{m_a} \frac{\partial \mathcal{S}_a}{\partial q_a} \right) \right)$$

Which is clearly a modified particle conservation equation CE. Note how if $\text{Im}\{W(q_a, t)\} = 0$ then we get the common continuity equation, which would mean that probability is conserved, and the solution $\Phi(q_a, t)$ would preserve its norm at all times (the conditional r_a^2 would integrate a same norm at all times in its spatial dimension q_a). Nonetheless, if $\text{Im}\{W(q_a, t)\} \neq 0$, then particles/probability are NOT conserved, and their source or sink will be quantified by $\frac{2a^2}{\hbar} \text{Im}\{W(q_a, t)\}$. Therefore, the norm of $\Phi_a(q_a, t)$ will not need to be preserved in the time evolution.

If W has that shape, $\Phi_a(q_a, t)$ will be the solution of the non-linear differential equation:

$$i\hbar \frac{\partial \Phi_a(q_a, t)}{\partial t} = -\frac{\hbar^2}{2m} \frac{\partial^2 \Phi_a(q_a, t)}{\partial q_a^2} + W(q_a, t)\Phi_a(q_a, t)$$

which if $\text{Im}\{W\} = 0$ we could say that is a single particle SE. Still, we can further develop the expression of W using the conditional definition of Φ_a . Carefully evaluating $\Phi_a(q_a, t) = \Psi(q_a, t; \vec{q}_b(t))$ defined in (SPCWF) and applying the chain rule we will get $\forall a \in \{1\dots n\}$ the expression of their $W(q_a, t) = \mathbb{W}(q_a, t; \vec{q}_b(t))$. For the real part:

$$\begin{aligned} \text{Re}\{W(q_a, t)\} &= \text{Re}\{\mathbb{W}(q_a, t; \vec{q}_b(t))\} = \\ &= -\frac{1}{2m_a} \left(\frac{\partial S(q_a, t; \vec{q}_b(t))}{\partial q_a} \right)^2 + \frac{\hbar^2}{2m_a R(q_a, t; \vec{q}_b(t))} \frac{\partial^2 R(q_a, t; \vec{q}_b(t))}{\partial q_a^2} - \frac{\partial S(q_a, t, \vec{q}_b(t))}{\partial t} = \\ &= -\frac{1}{2m_a} \left(\frac{\partial \mathcal{S}_a(q_a, t)}{\partial q_a} \right)^2 + \frac{\hbar^2}{2m_a \mathbf{r}_a(q_a, t)} \frac{\partial^2 \mathbf{r}_a(q_a, t)}{\partial q_a^2} - \left(\frac{\partial S(q_a, t, \vec{q}_b)}{\partial t} \Big|_{\vec{q}_b(t)} + \sum_{k=1; k \neq a}^n \frac{\partial S(q_a, t, \vec{q}_b)}{\partial q_k} \Big|_{q_k(t)} \frac{dq_k(t)}{dt} \right) \end{aligned}$$

Note how the only terms introducing some coupling with the rest of particles are the last two. They are the source of the **entanglement**, **exchange** and **correlations** with the rest of the dimensions.

Now, knowing that the full wave-function follows the **SE** and thus the **QHJE**, we can evaluate the expression for $\frac{\partial S(q_a, t; \vec{q}_b)}{\partial q_k}$ in the equation above:

$$\begin{aligned} Re\{W(q_a, t)\} &= Re\{\mathbb{W}(q_a, t; \vec{q}_b(t))\} = \\ &- \frac{1}{2m_a} \left(\frac{\partial \mathcal{S}_a(q_a, t)}{\partial q_a} \right)^2 + \frac{\hbar^2}{2m_a} \frac{\partial^2 \mathbf{r}_a(q_a, t)}{\partial q_a^2} - \sum_{k=1; k \neq a}^n \left(\frac{\partial S(q_a, t, \vec{q}_b)}{\partial q_k} \Big|_{q_k(t)} \frac{dq_k(t)}{dt} \right) + \\ &+ \sum_{k=1}^n \left[\frac{1}{2m_k} \left(\frac{\partial S}{\partial q_k} \Big|_{\vec{q}_b(t)} \right)^2 - \frac{\hbar^2}{2m_k R} \frac{\partial^2 R}{\partial q_k^2} \Big|_{\vec{q}_b(t)} \right] - V(q_a, t; \vec{q}_b(t)) \end{aligned}$$

Observe that in the last sum, the $k = a$ term is equal to the two initial terms, which cancel each other out and we are left with the final expression (ReW)(where we made the potential energy absorb the negative sign, just for convenience):

$$Re\{\mathbb{W}(q_a, t; \vec{q}_b(t))\} = \sum_{k=1; k \neq a}^n \left[\frac{1}{2m_k} \left(\frac{\partial S}{\partial q_k} \Big|_{\vec{q}_b(t)} \right)^2 - \frac{\hbar^2}{2m_k R} \frac{\partial^2 R}{\partial q_k^2} \Big|_{\vec{q}_b(t)} - \frac{\partial S}{\partial q_k} \Big|_{q_k(t)} \frac{dq_k(t)}{dt} \right] + V(q_a, t; \vec{q}_b(t))$$

We now have defined $Re(W)$ without using Φ_a in the same definition (necessary if we want to use the Schrödinger like equation computationally). Note how it is in here where the entanglement with the rest of dimensions emerge.

For convenience let us decompose the potential V into terms concerning q_a and terms that do not contain an explicit dependence on q_a (constant terms in $V(q_a, t; \vec{q}_b(t))$):

$$V(q_a, \vec{q}_b, t) = \mathcal{U}_a(q_a, \vec{q}_b, t) + \mathcal{U}_b(\vec{q}_b, t)$$

We will define two potential energies out (4). On the one hand, we have the “traditional” conditional potential for q_a , \mathcal{U}_a : which introduces geometric correlations with the rest of coordinates. On the other hand, we have a potential term due to the presence of the rest of particles in the system (the effect of the environment): the quantum correlation potential, which we will call G_a :

$$G_a(q_a, t; \vec{q}_b(t)) := \mathcal{U}_b(\vec{q}_b, t) + \sum_{k=1; k \neq a}^n \left[\frac{1}{2m_k} \left(\frac{\partial S}{\partial q_k} \Big|_{\vec{q}_b(t)} \right)^2 - \frac{\hbar^2}{2m_k R} \frac{\partial^2 R}{\partial q_k^2} \Big|_{\vec{q}_b(t)} - \frac{\partial S}{\partial q_k} \Big|_{q_k(t)} \frac{dq_k(t)}{dt} \right]$$

Performing the same development for the imaginary part of W , that is, evaluating the definition of **SPCW** in $Im\{W(q_a, t)\}$ and applying the chain rule:

$$\begin{aligned} Im\{W(q_a, t)\} &= Im\{\mathbb{W}(q_a, t; \vec{q}_b(t))\} = \\ &\frac{\hbar}{2R^2} \Big|_{\vec{q}_b(t)} \left(\frac{\partial R(q_a, t; \vec{q}_b(t))^2}{\partial t} + \frac{\partial}{\partial q_a} \left(\frac{R^2}{m_a} \frac{\partial S(q_a, t; \vec{q}_b(t))}{\partial q_a} \right) \right) = \\ &\frac{\hbar}{2R^2} \Big|_{\vec{q}_b(t)} \left(\frac{\partial R(q_a, t, \vec{q}_b)^2}{\partial t} \Big|_{\vec{q}_b(t)} + \sum_{k=1; k \neq a}^n \frac{\partial R^2}{\partial q_k} \Big|_{\vec{q}_b(t)} \frac{dq_k(t)}{dt} + \frac{\partial}{\partial q_a} \left(\frac{R^2}{m_a} \frac{\partial S(q_a, t; \vec{q}_b(t))}{\partial q_a} \right) \right) \end{aligned}$$

As the whole wave-function follows the **SE**, we have an expression for the n-particle continuity equation **CE**, which evaluating at $\frac{\partial R(q_a, t, \vec{q}_b)^2}{\partial t}$ and noting there is a cancellation of the $k = a$ term (as happened with the real case), we arrive at the expression independent of Φ_a :

$$Im\{\mathbb{W}(q_a, t; \vec{q}_b(t))\} = \frac{\hbar}{2R^2} \Big|_{\vec{q}_b(t)} \sum_{k=1; k \neq a}^n \left[\frac{\partial R^2}{\partial q_k} \Big|_{\vec{q}_b(t)} \frac{dq_k(t)}{dt} - \frac{1}{m_k} \frac{\partial}{\partial q_k} \left(R^2 \frac{\partial S}{\partial q_k} \right) \Big|_{\vec{q}_b(t)} \right] \quad (\text{ImW})$$

We will define the potential energy term $J_a(q_a, t; \vec{q}_b(t)) := Im\{\mathbb{W}(q_a, t; \vec{q}_b(t))\}$.

Then we have that the complex potential is decomposed in the following potential terms:

$$W(q_a, t) = \mathbb{W}(q_a, t; \vec{q}_b(t)) = \mathcal{U}_a(q_a, t; \vec{q}_b(t)) + G_a(q_a, t; \vec{q}_b(t)) + i J_a(q_a, t; \vec{q}_b(t))$$

In a nutshell, we have decomposed the n dimensional **SE** into a **system of n coupled Single Particle Pseudo-Schrödinger Equations** (PSE). For each $a \in \{1..n\}$ and $\vec{q}_b = \vec{q} \setminus q_a$:

$$\begin{aligned} i\hbar \frac{\partial \Phi_a(q_a, t)}{\partial t} &= \left[\frac{\hbar^2}{2m_a} \frac{\partial^2}{\partial q_a^2} + \mathcal{U}_a(q_a, t; \vec{q}_b(t)) + G_a(q_a, t; \vec{q}_b(t)) + i J_a(q_a, t; \vec{q}_b(t)) \right] \Phi_a(q_a, t) \quad (\text{PSE}) \\ \frac{dq_a(t)}{dt} &= v_a(q_a, t) = \frac{1}{m_a} \frac{\partial \mathcal{S}_a(q_a, t)}{\partial q_a} \end{aligned}$$

Given an initial whole wave-function $\Psi(\vec{q}, t = t_0)$ and an initial point for the trajectory of the system $\vec{q}(t = t_0) = \vec{q}_0 \in \mathbb{R}^n$, one could define the n initial SPCWF-s Φ_a . Their evolution would be coupled: each time step in the equation of the a -th SPCWF, one needs to evaluate the trajectory of the rest of coordinates. The funny point is that the development is powerfully based on a Bohmian like interpretation of QM, but it does not matter if one accepts Bohmian trajectories or not, the coupled system is **exactly** equivalent to the n dimensional **SE**.

Another interesting point is that, in a quantum system, in general it is impossible to treat the dynamics of one particle without considering the rest, due to the quantum potential **Q**. Nonetheless, here, we have developed a way in which we can treat one particle aside from the rest of the system (the environment), all the effect of which has been packed in the G_a and J_a potential energy terms. This is something Orthodox mechanics fails to satisfactorily offer, but it turns out to be a natural consequence of Bohmian Mechanics.

Most importantly, this means that we are now allowed to make approximations in the single dimension scale! That is, as a function of the nature of each particle in the system, *ad hoc* approximations can now be done (which using the n dimensional Schrödinger Equation was not possible -everything was mixed up together).

Now, one could initially think that this approach allows the evolution of trajectories of the quantum system without the wave-function! In Sections 1 and 2, it seemed like the trajectories were something *a posteriori*: one needed to know the whole wave-function and only after that, one could obtain the piloted trajectory. And that is why one could perhaps take them as an unnecessary *add on* in the quantum machinery. But in this case, the whole wave-function appears to have faded away: now the computation of the trajectories has become central. The point is that this is not fully honest: in order to obtain the expressions of G_a and J_a , we still need to know the whole wave-function. So in reality, the problem is still there, just that it is a bit more concealed. This is because, once one conditions the full wave-function to a particular position in some of the coordinates, the operation cannot be reversed! That is, even if we know the expression for $\Phi_a \forall a \in \{1\dots n\}$, we are not able to “rebuild” the whole wavefunction from there. And if one looks at the expression of the potentials, we still need it in each time iteration.

We should not be discouraged at this point though, because new algorithmic approaches can be built on this grounds. For instance a first idea one could think of would be the following: given an initial full wavefunciton, evolve in parallel several trajectories with initial position according to the initial probability density. In each time step, use the trajectories in order to rebuild the full wave-function in that new time, which could be used to obtain the values of G_a and J_a for the new time and feed back the algorithm. The mesh of trajectory positions approximates the density of particles and the phase could be rebuilt by noting that the several trajectory velocities will give information of the original n particle velocity fields. The unfortunate point with this approach is that in the end we would require the parallel computation of many many trajectories, exponentially more for each increasing dimension. That is, we would fall again in the *impasse* of trying to solve exactly the **SE**. Just like what happened with the CN approach. Instead, we could try to apply approximations that still capture all the physics but make the coupled system way easier. For instance, expanding G_a and J_a in a Taylor series around the evolving particle, or using a Born-Huang expansion of the whole wave-function, as exposed in Section 3. Thus, similar to the work on DFT, *the theory is exact, but the solutions need to be approximate*.

Finally, let us emphasize the role of the potential terms \mathcal{U}_a , G_a and J_a :

- \mathcal{U}_a : It is a real potential whose explicit expression is known, it is the sum of potential energy terms concerning q_a . It accounts for the classical “geometrical” constrictions across the coordinates. $\mathcal{U}_b(t; \vec{q}_b)$, is just the sum of terms that do not concern a_a . It is a constant in space.
- G_a : It is a real potential. Its explicit dependence of on q_a is unknown, unless the whole wavefunction is known. It takes into account most of the quantum entanglement and correlation.
- iJ_a : It is a complex potential. Its explicit expression is unknown in the same way as G_a ’s. It takes into account that the norm of a conditional wave-function does not need to be conserved. It will be the source and sink term of probability density.

References

- [1] X.Oriols, J.Mompart,*Applied Bohmian Mechanics: From Nanoscale Systems to Cosmology* Pan Stanford, Singapore (2012)
- [2] D. Bohm, *A Suggested Interpretation of the Quantum Theory in Terms of "Hidden" Variables. I*, Physical Review,85, 166 (1952); D. Bohm,*A Suggested Interpretation of the Quantum Theory in Terms of "Hidden" Variables. II*, Physical Review,85, 180 (1952)
- [3] Frederick W. Byron, Robert W. Fuller, *Mathematics of Classical and Quantum Physics, Volume 1*, Dover Publications; Revised ed. edition (August 20, 1992)
- [4] Yuval Grossman, Problem Set 1 (<https://www.classe.cornell.edu/~yuvalg/p4444/hw1-sol.pdf>) - *Introduction to Particle Physics Course: Spring 2017* (CLASSE)
- [5] Holland P R 1993 *The Quantum Theory of Motion* (Cambridge: Cambridge University Press) Ch.8
- [6] Bohm D and Bub J 1966 *A proposed solution of the measurement problem in quantum mechanics by a hidden variable theory* Rev.Mod. Phys.38 453
- [7] Benseny A, Tena D and Oriols X 2016 *On the classical Schrödinger equation* Fluct. Noise Lett. 15 1640011 arXiv:1607.00168
- [8] E. Madelung, *Quantentheorie in hydrodynamischer Form*, Zeitschrift fur Physik 40, 322 (1926)
- [9] Chapter 19.2 of W. H. Press, S. A. Teukolsky, W. T. Vetterling, and B. P. Flannery, *Numerical Recipes: The art of Scientific Computing* (Cambridge, 1992).
- [10] Trefethen, Lloyd N.; Bau, David (1997), *Numerical linear algebra*, Philadelphia: Society for Industrial and Applied Mathematics, ISBN 978-0-89871-361-9
- [11] A. George and E. G. Ng (1988), 'On the complexity of sparse QR and LU factor-ization of finite-element matrices', SIAM J. Sci. Comput. 9, 849–861.
- [12] D. Dürr, S. Goldstein, and N. Zanghi, *Quantum Equilibrium and the Origin of Absolute Uncertainty*, Journal of Statistical Physics 67(5–6), 843 (1992)
- [13] M. H. Bramhall and B. M. Casper. *Reflections on a Wave Packet Approach to Quantum Mechanical Barrier Penetration*. Am. J. Phys., 38(9):1136–1145, 1970.
- [14] Oriols X. 2007 *Quantum-trajectory approach to time-dependent transport in mesoscopic systems with electron-electron interactions* Phys. Rev. Lett. 98 066803
- [15] Albareda G, Kelly A, Rubio A. *Nonadiabatic quantum dynamics without potential energy surfaces*. Phys Rev Materials. 2019; 3: 023803.
- [16] Oriols X and Benseny A 2017 *Conditions for the classicality of the center of mass of many-particle quantum states* New J. Phys. 19 063031